UNIVERSIDADE
BEIRA INTERIOR

Rapid and selective capture of nucleic acids using carbon nanotubes

Pedro Filipe Lopes Ferreira

Dissertação para obtenção do Grau de Mestre em
Biotecnologia
(2º ciclo de estudos)

Orientador: Profª. Doutora Fani Pereira de Sousa
Co-orientador: Doutora Ana Paula Mora Tavares
Co-orientador: Profª. Doutora Mara Guadalupe Freire Martins

janeiro de 2021

“Come what may”

To all the special people that made it possible.

Acknowledgments

This past year has been an incredible learning journey. Looking back, I see how much I have grown, not only professionally but also in personal terms. In addition to the knowledge I acquired, I had the opportunity to meet and work with incredible people who helped me achieve this goal, to whom I would like to express my gratitude.

First, I would like to thank Professor Fani who did not hesitate to welcome me into the research group, and who supported me from the very first moment. Since the beginning of my academic career, the teacher has been a mentor, always motivating me to give everything and to always look for more. With the teacher, I have already achieved much more than I would anticipate and have learned many things that I will take with me for life. This work would not have been possible without your dedication, perseveration, and scientific knowledge. Also, I would like to thank Professors Ana Tavares, Mara Freire, and Cláudia Silva, who were always promptly available to help. You were a huge help, and together I would like to continue improving and moving forward with our work.

I would also like to thank my fantastic lab group, who welcomed me very well in the laboratory and was a fundamental part of my learning process. A special thanks to my partnér, who accompanied me on this long journey. We finally made it!

A gigantic thanks to all my friends, who have supported me since the beginning. I don't know why, but I was always lucky to find the best friends I could have, and you are all in my heart. I hope you will continue here for my next achievements and failures.

To all my family, and especially to my two incredible parents António Ferreira and Maria da Conceição Lopes, my major sponsors on this journey. You always gave everything to me and never gave up. I owe to you what I am today, and I hope I made you proud. A huge thanks to my dear brother, Luís Ferreira, who really wanted to have his name on this job. I leave you with the responsibility of achieving this position one day and that you do it more successfully. Love you with all my heart.

Finally, I would like to thank the most special person I met during this journey, Micaela Riscado. You were always there to support me in the most difficult moments and to celebrate the happiest moments, and you were there to help me whenever I needed it. I have no words to thank you for everything you did for me, and I hope that what this journey brought together, nothing else divides. You were responsible for everything that this work represents, and for that reason, I dedicate it to you.

Resumo alargado

A terapia genética tem-se destacado como uma das opções mais promissoras para o tratamento de doenças genéticas e adquiridas. Para isso, o DNA plasmídico recombinante (pDNA) deve ser recuperado de extratos complexos cuja composição compreende uma alta diversidade de biomoléculas que partilham características e propriedades semelhantes. Além disso, estas biomoléculas podem causar imunogenicidade, aquando da administração, sendo a sua remoção um pré-requisito fundamental na preparação de pDNA estável, de alta pureza e biologicamente ativo para aplicação terapêutica. Consequentemente, a purificação de pDNA é um processo muito dispendioso para a indústria farmacêutica, e apresenta também um grande impacto para o ambiente, devido ao uso de solventes orgânicos e sais. Para responder a este desafio e isolar o pDNA de extratos complexos, é proposta uma alternativa promissora, baseada no uso de nanotubos de carbono (CNTs). Devido à sua versatilidade, os CNTs têm sido amplamente explorados em diversas áreas, sendo que, as suas propriedades únicas, como o tamanho, forma, estrutura, biocompatibilidade e elevada afinidade por biomoléculas levaram a que nos últimos anos tenham também ganho muita relevância para aplicações biológicas.

Neste âmbito, o presente trabalho descreve o desenvolvimento de um método eficaz para isolar o pDNA a partir de um lisado complexo de *Escherichia coli*, utilizando nanotubos de carbono de paredes múltiplas (MWCNTs) para capturar proteínas e outros ácidos nucleicos contaminantes, como RNA e DNA genómico (gDNA).

Primeiramente, foram avaliados diferentes diâmetros de MWCNTs (<10 nm, <10/20 nm, 20/40 nm, 60/100 nm), paralelamente à realização de ensaios de *screening* de adsorção e de desorção de RNA. Misturas de RNA e pDNA foram também preparadas de forma a estudar a potencial seletividade na separação destas duas biomoléculas por parte dos MWCNTs. A captura de outros contaminantes foi avaliada através da aplicação de amostras mais complexas provenientes de lisado de *E. coli* aos MWCNTs, seguida pela quantificação das proteínas e do gDNA presentes na amostra. Para reduzir ainda mais o impacto ambiental desta tecnologia, a possibilidade de reciclagem e reutilização dos MWCNTs foi também estudada. Os resultados deste trabalho evidenciaram a capacidade dos MWCNTs em capturar com alguma seletividade o RNA de amostras complexas, possibilitando a clarificação rápida do pDNA. Os resultados também demonstraram que os MWCNTs podem reduzir a quantidade de impurezas no primeiro ciclo de extração,

reduzindo cerca de metade das proteínas, e reduzindo também significativamente os níveis de gDNA em solução, com uma taxa de recuperação de 86% de pDNA. Após 3 ciclos consecutivos, a pureza do pDNA solúvel aumentou significativamente. Por último, e de forma a averiguar a biossegurança na utilização dos MWCNTs, foi avaliada também a sua toxicidade em linhas celulares humanas, ao longo de 48 h. Através deste ensaio, ficou comprovado que os MWCNTs não apresentam qualquer toxicidade para as linhas celulares usadas, nomeadamente fibroblastos humanos.

Assim, os resultados obtidos demonstram que foi possível desenvolver um método simples, eficiente e confiável para a purificação rápida de pDNA.

Palavras-chave

Biofármacos; DNA plasmídico; Extração de fase sólida; Nanotubos de carbono; RNA; Separação de ácidos nucleicos.

Abstract

Gene therapy is raising as one of the most promising options for treating genetic and acquired disorders. However, recombinant plasmid DNA (pDNA) must be recovered from complex extracts with a diversity of biomolecules that share similar characteristics and properties. Moreover, those biomolecules can cause immunogenicity, and their removal is a fundamental prerequisite in preparing high-purity, stable, and biological active pDNA for therapeutic application. To respond to this challenge and isolate pDNA from complex extracts, a promising alternative is proposed, based on using carbon nanotubes (CNTs). In recent years, biological applications of CNTs have been explored, motivated by their interesting size, shape, structure, biocompatibility, and high affinity for biomolecules.

In this work, an effective method to isolate pDNA was developed, using multi-walled carbon nanotubes (MWCNTs) to capture proteins and other contaminating nucleic acids, like RNA and genomic DNA (gDNA). MWCNTs with different diameters were evaluated, while mixtures of RNA and pDNA were prepared to address the selectivity of the material. The results of this work evidenced the ability of MWCNTs to capture RNA from complex samples, enabling the clarification of pDNA. The results also demonstrated that MWCNTs can reduce the amount of impurities in the first cycle of extraction, reducing about half of the proteins, and significantly reducing the levels of genomic DNA in solution, with a pDNA recovery rate of 86%. When performing up to three consecutive cycles, the purity of soluble pDNA can be significantly improved.

To further reduce the environmental impact of this technology, the possibility of recycling CNTs has also been confirmed, as well as it was assured the safety on their use by verifying the biocompatibility of this material. Thus, attained results demonstrate the development of a simple, efficient, and reliable method for rapid purification of pDNA biopharmaceuticals.

Keywords

Biopharmaceuticals; Carbon nanotubes; Nucleic acids isolation; Plasmid DNA; RNA; Solid-phase extraction

Table of Contents

List of Figures

List of Tables

List of Acronyms

AAVS	Adeno-associated viruses
ATPS	Aqueous two-phase system
CCVD	Catalytic chemical vapor deposition
CD	Circular dichroism
CNT	Carbon nanotube
Cq	Quantitation cycle
CVD	Chemical vapor deposition
DMEM F-12	Dulbecco's Modified Eagle's Medium/Nutrient Mixture F-12
DMSO	Dimethyl sulfoxide
d-SPE	Dispersive solid-phase extraction
E. coli	*Escherichia coli*
EPA	Environmental Protection Agency
FBS	Fetal bovine serum
gDNA	Genomic DNA
hFIB	Human dermal fibroblasts
LLE	Liquid-liquid extraction
MEPs	Micro-extraction by packed sorbent
mRNA	Messenger RNA
MSPD	Matrix solid-phase dispersion
MTT	3-(4,5-dimethylthiazol-2-yl)-2,5-diphenyltetrazolium bromide
MWCNT	Multi-walled carbon nanotube
OD	Optical density
pDNA	Plasmid DNA
SBSE	Stir-bar sorptive extraction
SDS	Sodium dodecyl sulfate
siRNA	Small interfering RNA
SPDE	Solid-phase dynamic extraction
SPE	Solid-phase extraction
SPME	Solid-phase micro-extraction
SSA	Specific surface area
SWCNT	Single-walled carbon nanotube
UV	Ultraviolet

Scientific Communications

Oral Presentation

Pedro Ferreira, Cláudia G. Silva, Mara G. Freire, Ana M. Tavares, Fani Sousa. Rapid and selective capture of nucleic acids using carbon nanotubes. XV ANNUAL CICS-UBI SYMPOSIUM 2020. 1-2 October 2020, Covilhã, Portugal.

CHAPTER 1

1. Introduction

1.1. Nanotechnology and nanomaterials

The physicist Richard P. Feynman first suggested the concept of Nanotechnology during a lecture entitled "There's Plenty of Room at the Bottom" in 1959 [1]. He envisioned the possibility of rearranging atoms and molecules individually to create new and improved materials. Since then, scientists have been making progress in this area, and nowadays, it is undeniable the impact of nanotechnology in different fields, due to the possibility of developing a wide variety of materials at nanoscale with enhanced properties.

While the definition of "nanotechnology" is not consensual, according to the National Nanotechnology Initiative, nanotechnology can be referred to as the understanding, design, and development of structures whose size has been engineered at the nanometric scale [2]. These nanomaterials must have at least the dimension between 1 and 100 nm and be developed by top-down or bottom-up engineering of individual components. Owing to their unique properties, nanomaterials are expected to provide solutions to challenges in a wide range of fields, from biomedical applications to environmental sciences, increasing, therefore, our quality of life [3,4]. In fact, the use of nanotechnology for medical proposes has grown exponentially, accompanying the considerable technological advance, with the primary goal of successful testing and clinical approval of several nanomaterials [5]. Among these nanomaterials with potential on biomedical approaches, carbon nanotubes (CNTs) are increasingly gaining popularity as potential drug carriers [6–9], therapeutic agents [10–13], and diagnostic tools [14–16].

1.2. Carbon nanotubes

A new field of nanotechnology was further developed, in 1991, when the Japanese scientist Sumio Iijima and his coworkers reported the preparation of CNTs by using an arc-discharge evaporation method [17]. This new carbon allotrope sparked much attention from scientists due to their inherent unique properties such as high surface area, high aspect ratio (length to diameter), and ultralight weight [18]. CNTs are composed of graphene sheets rolled up to form tubular, needle-shaped structures with size in nanometric scale in diameter and several millimeters in length. Because each atom of carbon has three neighborhoods, CNT has a strong bond between C-C atoms (sp2 hybridization), making them very stable against deformations [18,19].

1.2.1. Classification and properties

Carbon nanotubes can have one or multiple graphene wall sheets, and therefore they can be classified as single-walled CNTs (SWCNTs) or multiple-walled CNTs (MWCNTs) (Figure 1).

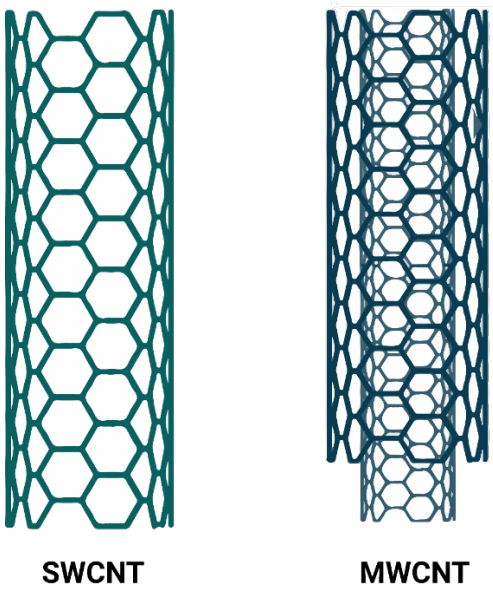

Figure 1 - Carbon nanotube structure according to the number of sheets.

SWCNTs are composed of a single graphene sheet with a diameter that comprises between 0.4 and 40 nm, whereas MWCNTs are composed of two to several sheets forming concentric cylinders with an interlayer distance of 0.35 nm, with diameters from 2 to 100 nm. Table 1 shows the main differences between SWCNTs and MWCNTs [19].

Table 1 - General properties of SWCNTs and MWCNTs (adapted from [20]).

SWCNTs	MWCNTs
Single layer of graphene	Multiple layers of graphene
A catalyst is required for synthesis	Can be produced without catalyst
Bulk synthesis is difficult	Bulk synthesis is easy
More defect during functionalization but easy to improve	Less defect but difficult to improve
Purity is poor	Purity is high
Less accumulation in body	More accumulation in body
Easy characterization and evaluation	Difficult characterization and evaluation

Another way that CNTs can be classified is based on the variations of tubular structures caused by the mode that molecule wraps into a cylinder form. Scientists working in the field have come up with a mathematical based nomenclature to describe the chiral vector. The chiral vector determines the two equivalents lattice sites, which when joined result in a nanotube, defining the circumference [20,21]. This classification is based on a pair of indices (n, m), which are sufficient to define any particular SWCNT. The values of n and m can be found by merely counting the hexagons that separate the C_h vector, following the unity vector a^1 first, and then a^2 [19]. For a better understanding, Figure 2 represents a schematic diagram of the basic parameters that define the structure of a CNT. Thus, nanotubes with a chiral vector (n, 0) are defined as zigzag nanotubes, as they exhibit a zigzag pattern of atomic configuration along the circumference (Figure 2a). The armchair nanotubes are represented in Figure 2c. These occur when the chiral vector is (n, n), and, in this case, the atoms form a pattern of an armchair throughout the circumference. All other nanotubes are defined as chiral nanotubes and have a chiral vector (n ≠ m and n ≠ 0), as represented in Figure 2b [22]. This nomenclature (n, m) is not just useful to identify and designate CNTs, but it can be related, to a certain extent, with the conductivity properties of the resulting CNT. Hence, when n−m is a multiple of 3, then the nanotube is described as 'metallic' or highly conducting nanotubes, and if not, then the nanotube is a semi-metallic or semiconductor [20]. Indeed, the electronic structure of CNTs has been studied theoretically, and the correlation with experimental studies has demonstrated the optical, electrical, and mechanical properties [23]. One example is the use of CNTs composites as solar cells. In 2009, Tung and co-workers developed graphene/CNT composites for high-performance transparent conductors and demonstrated their application in organic solar cell technology with an inexpensive and massively scalable methodology [24].

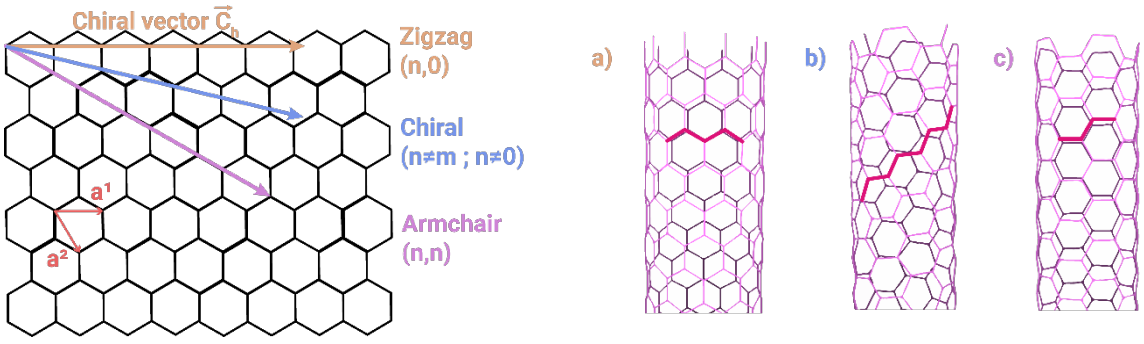

Figure 2 - Schematic diagram showing how a sheet of graphene is rolled to form a CNT with different chirality (a: Zigzag; b: Chiral; c: Armchair).

Because of their structural differences, SWCNTs and MWCNTs may have some variation in properties. Due to the multi-layer nature, MWCNTs have an outer wall that, apart from shielding the inner nanotube of chemical interactions, also gives high tensile strength properties. Moreover, carbon nanotubes also have a sp2 hybridization between the individual carbon bonds. This bond is stronger than the sp3 bond found in diamond, and theoretically, SWCNTs can even have tensile strength hundreds of times stronger than steel [20]. Also, due to the sp2 hybridization, each carbon is bound to three neighborhoods; thus, the fourth valence atom remains free in each unit, and these free electrons are delocalized over all atoms, providing excellent electrical and thermal conductivity properties. As a result of the strong bonds between carbons, CNTs can also withstand high temperatures [18].

Another great feature of CNTs is their elasticity. Studying CNTs under TEM and exposing them to great axial compressive forces has shown that these materials can bend and twist without damaging the nanotube, returning to the original form. Although, due to the defects in nanotubes structure (defects in atomic vacancies or resulting from rearrangement of the carbon bonds), CNTs elasticity has a limit, and under very powerful forces, it is possible to deform the shape of a nanotube temporarily. Table 2 shows the structural basis and main properties of SWCNT and MWCNT [20].

Table 2 - Structural basis of SWCNTs and MWCNTs.

Properties	SWCNTs	MWCNTs	References
Structure	Armchair, zigzag or chiral arrangement. Single graphite sheet is rolled round itself.	Graphite sheets are arranged in concentric layers	[25]
Electrical properties	Semiconducting or metallic	Semiconducting	[26]
Diameter range	0.4-2 nm	Inner tubes: 1-3nm Outer tubes: 2-100 nm	[27], [28]
Strength	Lower strength than MWCNTs	Stronger compared to SWCNTs	[29]

1.2.2. Synthesis and purification of CNTs

For the synthesis of CNTs various techniques are available, depending on carbon or energy source. Commonly, the production methods of SWCNTs and MWCNTs comprise three procedures: the carbon arc-discharge technique [30], the laser-ablation technique [31], and the chemical vapor deposition (CVD) technique [31]. The basis of these methods is the same, to form an individual or group of carbon atoms that can recombine to produce carbon nanotubes. Arc-discharge and laser-ablation are considered high-temperature techniques and were the first ones used to synthesize CNTs. Nonetheless, these techniques are not able to control the nanotube length, diameter, alignment, purity, density, and orientation of CNTs with accuracy; therefore, they have been substituted by low-temperature preparations (<800°C), like CVD [20].

Arc-discharge method is based on the energy transfer resulting from the interaction of two graphite electrodes and plasma and is widely used because it is the easiest way to synthesize CNTs, specially if the intended applications do not demand high structural accuracy. In this method, direct current is passed through the chamber, followed by the chamber pressurization and heating to approximately 4000 K. About half of the evaporated carbon solidifies on the cathode (negative electrode) tip in this procedure, and a deposit forms at a rate of 1 mm/min, whereas the anode (positive electrode) is consumed. The main advantage of arc-discharge technique is the ability and potential for the production of a large quantity of nanotubes [18]. On the other hand, as previously mentioned, the main disadvantage of this method is the limited control over the alignment (i.e., chirality) of the created nanotubes, which is essential for their

characterization and role. Additionally, this method mainly produces MWCNTs and requires a catalyst precursor (nickel, cobalt, and/or iron) to produce SWCNTs, and therefore purification of the final product is essential [20].

Laser ablation uses as energy source laser pulses that vaporizes a graphite target in a high temperature chamber. As described in the arc-discharge method, for the SWCNT production it is necessary to add metal particles as a catalyst to the graphite targets. Many parameters can influence the properties of CNTs synthesized by laser ablation method, such as the structural and chemical composition of the target material, the laser properties, the chamber pressure, among others [18]. The main advantage of this technique is the relatively high yield of CNTs synthesis, with low metallic impurities since metal particles tend to evaporate once the nanotube is closed, whereas the main disadvantage is that the obtained nanotubes are not necessarily straight and can have some branching. Also, the ablation method is not economically advantageous because it encompasses a need for great lasers power [18,22].

Chemical vapor deposition is one of the standard methods for the production of CNTs. There are many different CVD types, but for large scale synthesis of CNTs, catalytic chemical vapor deposition (CCVD) is the most widely used. It uses hydrocarbons like methane, benzene, or acetylene as carbon source, while high temperature provides enough energy for the decomposition of hydrocarbons over metal catalysts to form CNTs. As compared with laser ablation, CVD is an economically practical method for large-scale and produces high purity CNTs with an easier control of the reaction course. In Table 3 are presented the major differences between these techniques [18].

Table 3 - Comparison of the three major techniques for CNT synthesis.

	Arc-discharge method	Chemical vapor deposition	Laser ablation method
Yield Rate	>75%	>75%	>75%
SWCNT or MWCNT	Both	Both	Both
Advantages	Simple, inexpensive, high-quality nanotubes	Relatively high purity, room-temperature synthesis	Simple, low temperature, high purity, large-scale production, aligned growth possible
Disadvantages	High temperature, purification required, tangled nanotubes	Method limited to the lab-scale, crude product purification required	Synthesized CNTs are usually MWNTs, defects

During the synthesis, different MWCNTs and SWCNTs proportions and different diameters of nanotubes are produced. These factors lead to a problem since CNTs strongly interact with each other through van der Waals forces and have a tendency to occur in bundles. Even if CNTs of close diameter are produced, they frequently have widely different chirality. Besides, CNTs also have many impurities, consisting of graphene sheets, metal catalysts, amorphous carbon, and small fluorenes [18]. Therefore, methods to remove impurities and to further differentiate and isolate SWCNTs from MWCNTs, or CNTs of a particular chirality, had to be developed. Depending on the technique used for CNTs synthesis, there are different methods and procedures for the purification. The main steps that all purification procedures have to follow encompasses the deletion of large graphite particles and aggregates with filtration, dissolution in appropriate solvents to eliminate metal residues of the catalyst precursor (acid cleaning and thermal annealing), and fullerenes (use of organic solvents) [32,33]. In order to separate and remove amorphous carbon clusters, microfiltrations and chromatography are the most commonly used methods [20]. For the separation of SWCNTs by chirality, the methods used include density-gradient centrifugation combined with surfactant wrapping and gel chromatography [33].

1.2.3. Functionalization of CNTs

As referred, after the procedure of CNTs synthesis, the final sample comprises a mixture of CNTs with different diameters, lengths, and chirality properties. Additionally, many metallic impurities are found in the sample. Furthermore, due to their hydrophobic nature, nanotubes tend to agglomerate, forming bundles in most biocompatible solvents, therefore limiting their biomedical applications [34]. In order to solve these problems, functionalization emerges as the most effective approach. It is a chemical or physical modification process where desired functional groups or drug molecules are introduced onto the surface of CNTs. Besides being able to achieve high homogeneity, decrease toxicity, increase dispersibility and solubility, this process also allows other particular uses, like using CNTs for analytical purposes or as sensors [35].

There are multiple approaches for surface functionalization of CNTs, classified into two different methods: covalent or noncovalent functionalization. In covalent functionalization, chemical reactions are carried out, creating new chemical bonds and altering the original nanotube structure. This reaction will lead to the change of carbon sp2 hybridization to sp3 hybridization, causing the loss of the π-conjugation system of the graphene layer responsible for most of the optical, electrical, and thermal properties of CNTs [34]. Despite this drawback, covalent functionalization has given scientists the possibility to manipulate these structures that otherwise would be unattainable, providing an opportunity to develop CNTs with different characteristics, for different purposes through stable attachment of functional groups [36].

Noncovalent functionalization of CNTs is less robust and less controlled than covalent functionalization but provides an alternative way of tuning CNTs without affecting their structural integrity [35]. The responsible forces for the adsorption of molecules are π–π interactions, hydrogen bonds, and electrostatic interactions between the nanotube and the adsorbed molecule. As a result, noncovalent functionalization ensures the sp2-hybridized six-membered ring network and the extended π-conjugation, maintaining the physical, electric, thermal, and optical properties of CNTs. On the other hand, weaker interactions between CNTs and the functional groups come at the cost of a possible functional group detachment by pH modifications, temperature, or solvent change. This also could be an advantage as weaker bonding means that a reversible functionalization is possible, opening new doors for their use in biomedical applications [34]. Using this strategy, several molecules have been successfully adsorbed onto the surface of CNTs, such as small molecules like pyrene or porphyrin derivates [37], surfactants like sodium dodecyl sulfate or tween-20 [38], or biomolecules. Indeed, different biological molecules and macromolecules can be bound to the nanotubes, like polypeptides, phospholipids

[39], proteins [37], and nucleic acids [40]. Although a relatively unexplored area, bridging biological systems with CNTs is gaining biomedical research attention because of their promising pre-clinical possibilities [34]. In 2017, the research group of Tran described a method to immobilize DNA on the CNTs network to develop a DNA-based sensor to detect influenza A virus [41]. In 2011, Cuicui and co-workers explored the CNTs-protein interactions, through theoretical and experimental approaches, to investigate the interactions of SWCNTs with human serum proteins and observed a competitive binding of these proteins with different adsorption capacity. They also unveiled that the binding of blood proteins onto the surface of CNTs can significantly alter their cellular pathways and reduce cytotoxicity for these protein-coated SWCNTs [42].

1.2.4. Applications of CNTs

As anticipated before, perfect CNTs present some incredible features as high aspect ratio, high surface area, high tensile strength, low mass density, high heat conductivity, poor chemical reactivity, and high electron activity. However, while the properties described before are excellent per se, many of these nanoparticles can form secondary structures such as ropes, fibers, and thin films, all with their specific properties [19,22]. In the last years, many studies have suggested that these properties make CNTs potential candidates for an infinite variety of applications. Below are encompassed some of the main CNTs applications described in the literature [33]:

- Specialized materials.
- Batteries and energy devices, mainly including Li batteries, supercapacitors, solar cells, and materials for hydrogen storage.
- Sensors, including electrochemically based sensors and biosensors.
- Drug delivery.

1.2.4.1. Biomedical applications

The capacity of CNTs to be conjugated with different molecules or compounds like polymers, proteins, and nucleic acids, and their needle shape that permits them to cross biological membranes and access cells in an affordable way, makes these structures very interesting in the biomedical field. Nonetheless, three barriers need to be overtaken

in order to maximize their potential in biomedicine: functionalization, pharmacology, and toxicity of CNTs [20].

The lack of solubility in aqueous media is one of the main disadvantages of CNTs. Due to their highly hydrophobic surface, CNTs tend to form bundles and aggregate, and to overcome this problem, researchers have been modifying their surface, functionalizing CNTs with hydrophilic molecules to enhance their solubility and dispersibility, improving their biocompatibility [34]. Another barrier with CNTs is pharmacokinetics. Their biodistribution and pharmacokinetics depend on their physicochemical characteristics, like shape, size, chemical composition, aggregation, solubility, and functionalization. Thus, a deep understanding of the CNTs properties is required in order to modulate their distribution in the organism, after administration [20]. Also, the functionalization process can also help CNTs to gain more targeted delivery routes, enhancing their biomedical features. Another critical barrier is CNTs toxicity, which can also be influenced by various factors, being the size one of the most relevant ones. Particles under 100 nm have potentially harmful properties such as toxicity to the lung, escape from the normal phagocytic defenses, modification of protein structure, and activation of inflammatory and immunological responses [3]. However, the results of CNT toxicologic assays found in the literature seem to be somehow contradictory. In general, water-insoluble CNTs showed that they could induce a higher cytotoxicity, especially the ones presenting smaller sizes. In 2011, Cuicui research group explored CNTs-protein interactions, through theoretical and experimental approaches, to investigate the interactions of SWCNTs with human serum proteins and observed a competitive binding of these proteins with different adsorption capacities. They also unveiled that the binding of blood proteins onto the surface of CNTs can significantly alter their cellular pathways and reduce cytotoxicity for these protein-coated SWCNTs. Interestingly, through noncovalent binding of Bovine Fibrinogen (BFG), CNTs did not demonstrate toxicity, whereas non-functionalized CNTs showed approximately 40% of cytotoxicity [42].

Regarding the application of CNTs for diagnosis purposes, Richard and co-workers have studied the functionalization of MWCNTs by adsorption of amphiphilic gadolinium (III) chelate obtaining a stable paramagnetic contrast agent (CA) that could be used magnetic resonance imaging [43].

On the other hand, many reports have studied CNTs either as drug carriers and delivery systems, to facilitate the treatment of many devastating pathologies, like cancer and neurodegenerative diseases. Taghavi research team used the tubular structure of nanotubes to attach RNA, thus modulating the expression of specific genes, achieving

cancer cell death. They functionalized SWCNTs with AS1411 aptamer as a ligand to target tumor cells and with DOX and small interfering RNA (siRNA) molecules to perform chemotherapy and gene therapy. The result of this study was an increased cell death in a model of human gastric cancer when compared to the individual CNT-based treatments or with free DOX [44].

Although CNTs have some inconveniences that need to be overcome, the versatility of CNTs for biomedical applications is enormous. They can be used as a theragnostic tool, combining the disease detection and treatment capacity at the same time. Also, these structures can be used in diagnosis as efficient biosensors or CA for non-invasive imaging, and at the same time, increase the lifetime of drugs in the organism, facilitate their direct delivery to target tissues. All this makes CNTs an auspicious system, with an enormous application potential.

1.3. Biopharmaceuticals

Biopharmaceuticals (or biologics) are therapeutic products manufactured from biological sources like human cells, animals, or microorganisms and include protein-, nucleic acid-, and cell-based products [45]. Unlike traditional drugs synthesized by chemical processes, biopharmaceutical products result from biological processes, in which cells or organisms are genetically modified to produce molecules of interest [46]. Over the past years, biopharmaceuticals are pushing the frontiers of science and research, and its industry has provided significant value to society with the development of several innovative therapeutics. Indeed, since the production of recombinant human insulin in 1982, biopharmaceuticals have revolutionized health care, changing the paradigm of life-threatening diseases that were medically untreatable [47]. From 2014 to 2018, 155 biopharmaceutical products have received approval in the United States and European Union, across a wide variety of disease areas, corresponding to 52% of genuinely new products on the market [48].

Through proteins, antibodies, cells, and gene-based products, biopharmaceuticals can successfully treat diseases by demonstrating biological activity and performing specific functions. Compared with chemical drugs, biopharmaceuticals have higher selectivity and low non-specific toxicity, but they also have a higher cost [46]. Biotechnological processes used in biopharmaceuticals production are complex and costly to design, develop, construct, and operate. However, an increase in biotechnology research is being incorporated into the largest pharmaceutical companies to improve and optimize the process [49].

From the identification of drug targets and receptor molecules to find the appropriate strategies for producing biological molecules, several fields must work together and interact to develop a biopharmaceutical process. Following these steps, the production yield and product characteristics are optimized, and the biomolecule is expressed recombinantly. The whole process needs to be reproducible and feasible in the technical-economic aspect, and the therapeutic molecule needs to meet the specified quality to enter the market [49]. It is of the utmost importance that the biopharmaceutical product meets the standards set by regulatory agencies to have practical value [45].

To respond to the current increase in product demand, there is a necessity for the development of less expensive products increasing their competitiveness. Thus, innovation in technological tools as well as production processes are to be pursued to improve the production process [50].

1.3.1. Biopharmaceutical production

A straightforward approach of the main steps and the challenges that constitute the biopharmaceutical production process is described in the following topics. The manufacturing of biopharmaceuticals encompasses two main stages: the upstream and downstream processing [49] (Figure 3). Upstream processing comprises all the steps required to produce a compound by biotechnological means, which includes the cell line selection, culture media formulation, establishment of cultivation parameters (pH, temperature, and oxygen concentration), cultivation type (submerged, solid-state, batch, fed-batch, continuous, etc.), followed by inoculation, small scale cultivation, and manufacturing scale cultivation [49]. Then, downstream processing includes all the steps required to isolate and purify the target molecule from the production source, up to a point where the pre-established end-product specifications are met. This includes cell lysis (if required), refolding (if required), initial recovery, purification, and polishing [51]. Due to the process complexity and high purity required for biopharmaceuticals, downstream processing usually takes 60%-90% of the total production costs [52].

Over the years, a significant progress has been achieved by optimizing the upstream processing. Upstream depends mostly on biological limits and can be improved without a significant increase in costs. However, downstream processing was initially designed for small scale processes and thus lower amounts of product. By increasing the feed volumes entering the facilities of downstream processing the equipment reaches its physical limits, therefore resulting in an increase of processing time, material consumption and costs. The type and concentration of impurities can amplify the already

existing problem. Hence, new approaches for optimized strategies and technology are necessary [47].

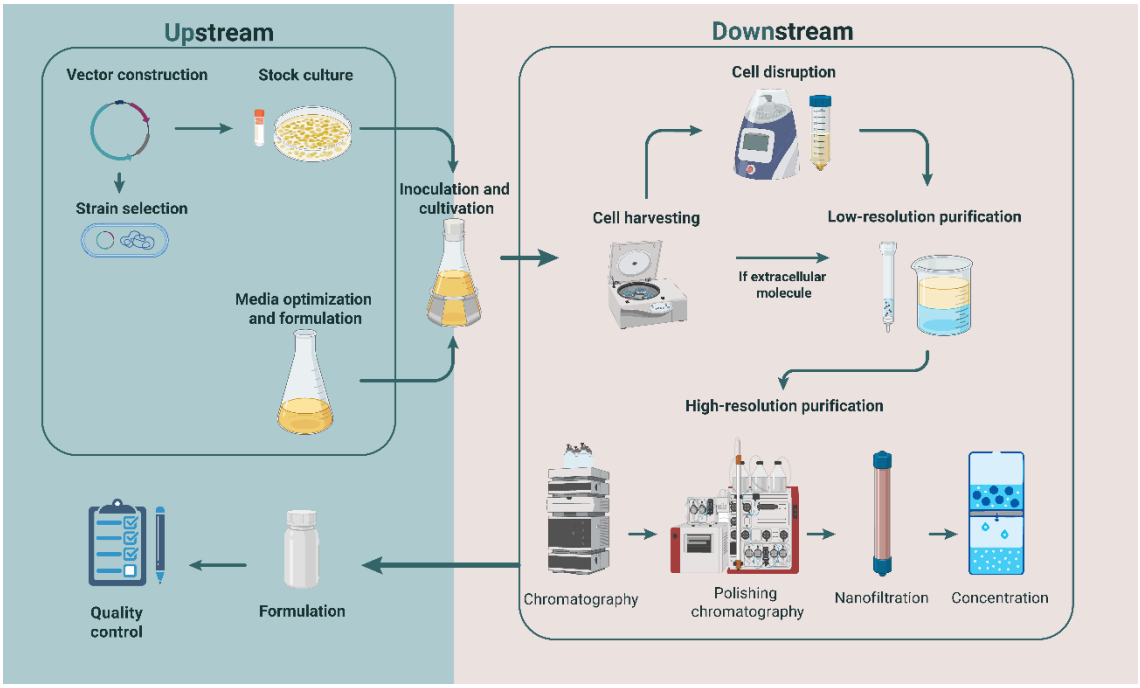

Figure 3 - Common upstream and downstream procedure used in biopharmaceutical manufacture.

1.3.1.1. Upstream processing

The main objective of the recombinant production of biopharmaceuticals is undoubtedly to optimize the product yield, in the upstream stage. The higher product concentration is usually associated to fewer steps in the downstream processing operations, thus reducing the costs [45]. Depending on the expression system chosen, different unit operations can be selected. Over the last years, upstream processing observed significant progress mainly due to increased cell culture understanding [50]. In the upstream stage, the most important aspects to be developed are the cell line used, media composition, operation strategy (batch, fed-batch, continuous cultivation, etc.), bioreactor design, process monitoring (pH, dissolved oxygen, temperature, nutrient concentrations, etc.), and product analytics (DNA detection, aggregates, endotoxins, lipopolysaccharide, virus, host cell protein concentration, etc.) [49].

Biopharmaceutical products are usually produced by microbial (e.g. *E. coli* or yeasts) or mammalian cells. However, there is a trend towards using mammalian-based expression systems, since there is an increase in the percentage of biomolecules that require posttranslational modifications, particularly glycosylation [45,50].

1.3.1.2. Downstream processing

Recovery, separation, and purification of products are essential in bioprocess engineering, since fermentation broths and cell cultures are complex, comprising an aqueous mixture of cells, with soluble extracellular or intracellular products [52]. Due to the high purity required for biopharmaceuticals, downstream processing is possibly the most challenging stage of biopharmaceutical manufacturing. Thus, to design an efficient downstream process, it is crucial to select the most appropriate techniques, optimize their performance, and combine them in a rational way to maximize yield and purity in the smallest number of steps [53]. Despite the lack of a universal purification strategy, the experience accumulated over the years with different bioproducts can be manifested into a general guideline of operations [47]:

1. Remove the most plentiful impurities first (i.e., separate cells from the culture medium first).
2. Remove the easiest and injurious impurities in early stages.
3. Make the most challenging and most expensive separations last (i.e., push chromatography toward the end of the downstream processing).
4. Select processes that exploit the most significant differences in the properties of the product and impurities (i.e., separate large from small, cationic from anionic, hydrophilic from hydrophobic, etc.).
5. Select processes that exploit different separation driving forces (i.e., do not use the same unit operation in a row).

Ultimately, the number and type of operations depend on the final use of the bioproduct. For instance, industrial enzymes usually require a purity of 80 to 90%, whereas for diagnostic proteins the required purity should be at least 95%, and a purity higher than 99.9% is often required for therapeutic applications [45]. Downstream processing can be divided broadly into three different stages: recovery, primary isolation, and polishing [47]. The first stage, recovery, aims to remove solids, release the product, and reduce the volume. Common operations are filtration, centrifugation and sedimentation [45]. The second stage, primary isolation, is the first line of purification, where the goal is to reduce the volume further and remove most impurities with properties different from those of the product. In this step, operations like solvent extraction, adsorption, precipitation, and ultrafiltration are commonly performed [47]. The final polishing section aims to remove the remaining impurities and unwanted forms of the product. Chromatography and adsorption are essential methods to accomplish the production of highly pure products [52]. One important factor that significantly affects the downstream train is

the location of the product during the production stage. Due to the need of cell disruption to recover intracellular products, more unit operations are usually required than that of extracellular products, leading to a higher amount of impurities. An additional solid-liquid separation is required for an intracellular product to remove the cellular debris produced due to cell disruption. In this case, the supernatant is then kept for further processing. For extracellular products, after cell removal, the supernatant can be purified directly since it is a less complex sample [47].

Being the recovery step the main focus of this study, will be addressed in more detail in the next topics.

1.4.Intermediate recovery

The starting point of intermediate recovery is usually a complex lysate stream in which the product is diluted, and this process has the primary objective of further purify and concentrating the biopharmaceutical product [45]. This complex lysate contains a significant fraction of genomic DNA (gDNA), large amounts of RNA and proteins, which together correspond to more than 90% of the total mass of solutes that remain in the clarified lysates. The contaminants should be substantially cleared in order to end up with a solution where more than 50% of the solutes are biopharmaceutical products [47]. Once this goal is achieved, the burden imposed on the last stage of the downstream process related to high-cost unit operations (typically chromatography) will be significantly reduced [50]. The clarified lysate entering the intermediate stage can be processed by several unit operations including membrane filtration, liquid-liquid extraction, precipitation, and adsorption. The choice of technique is usually dictated by the nature of the product, with minimal losses of product activity [45].

1.4.1. Membrane processing

Compared with other methods, membrane-based separations are a cost-effective, environmentally friendly, and straightforward method. This method is one of the most popular operations to reduce the volume and concentrate the sample [45]. The membrane itself acts like a selective barrier that separates two-phases and restricts the passage of some biomolecules or compounds larger than the pore size while allowing the passage of the smaller molecules [50]. Apart from the simplicity of this method, a wide range of membranes are commercially available for any specific process need.

Membrane separation was initially performed with a perpendicular feed through the membrane. This operation mode is prone to deposition and blockage of particulate in the pores of the filter and consequently reducing the permeate flow. An alternative solution is to flow the feed stream tangential to the membrane surface, providing enough sheer

force and avoiding particles to settle on or within the membrane structure [52]. However, tangential flow still suffers from two recurrent problems, concentration polarization, and membrane fouling. Concentration polarization results from the buildup of tangentially flowing stream near the membrane surface, increasing the local concentration leading to a gel layer formation. Though this layer is mainly aqueous, it can form physical and chemical bonds between the different solutes. Therefore, extra resistance is formed, leading to a reduction of the filtration flow rate, increasing the rejection of macromolecules. A series of physical and chemical processes can then be used to clean the gel layer and fully restore filtration fluxes [45]. On the other hand, fouling is characterized by a series of events that collectively lead to material deposition on the membrane surface. This phenomenon can lead to complete blockage of membrane pores in a way that the permeation flux is reduced beyond reasonable. Contrary to concentration polarization, fouling is an irreversible phenomenon and leads to membrane deterioration [47].

1.4.2. Precipitation

Precipitation is an effective method that allows the separation of biological products from complex media. The operation typically involves the addition of a precipitation agent (salts, organic solvents, nonionic polymers, polyelectrolytes, metallic ions, and affinity ligands), which decreases the solubility of solutes down to a point where self-association of molecules, aggregation, and precipitation set in [45,47]. This method is more effective as a concentration process rather than a purification one; therefore, precipitation is typically used early in the isolation of a biological product, reducing the volume to be processed [45]. Although it is easy to scale up the process, precipitation has some crucial drawbacks too. First, most of the equipment necessary to implement the process at a large-scale are costly, and on the other hand, the redissolution of sediments containing the bioproduct may be challenging to accomplish [47,50].

1.4.3. Liquid-Liquid extraction

Liquid-liquid extraction is a well-known process in the chemical and biotechnological industry, and for many years it was used to isolate biomolecules using solvents like phenol, chloroform, and isoamyl alcohol to remove impurities from lysates [47]. This type of extraction is advantageous since it is possible to remove most impurities by exploring the differential partitioning of bioproducts and impurities between two immiscible phases: the feed phase (usually aqueous), which contains the product, and the extractive phase (solvent) [52]. Aqueous two-phase systems (ATPS) are also attractive for industrial implementation owing to the ease of scaling and relatively simplistic equipment and facility demands [45].

Despite that, most liquid-liquid extraction methods are incompatible with safety standards required for biopharmaceuticals production, mostly due to the toxic nature of the solvents involved. In recent years, efforts have been made to replace those solvents for materials with unquestionable safety profiles, like water-soluble polymers and a series of salts [47]. However, the large amounts of polymers and salts that have to be added to the process streams, makes this technology more expensive. Another shortcoming is that, in most cases, the bioproduct will be diluted, requiring the addition of a subsequent concentration step [54].

1.4.4. Adsorption

Adsorption uses solid particles, which can interact preferentially with certain impurities compared to the bioproduct, to reduce the amount of contamination present in the sample [47]. Many interactions can occur in a given adsorption method, such as van der Waals forces, electrostatic, hydrophobic interactions, to more specific covalent bonding. In most cases, the adsorbent particles are porous and with large surface areas to permit full adsorption of impurities and thus originate high binding capacities [55].

Two main methods for promoting contact between the process stream and the adsorbent particles are fixed bed or batch adsorption. In fixed bed, the particles are packed in a column, and the process stream is pumped until the capacity of the bed for the target impurities is used. The bound impurities are then eluted from the adsorbent particles by washing out the column with an appropriate buffer. Following an adequate washing and cleaning, the bed is equilibrated with the adsorption buffer and is ready for another adsorption cycle [56]. In batch adsorption, the adsorbent is added to a tank that contains the sample to be treated. After allowing adsorption of the solutes, solids are separated (e.g., by centrifugation or filtration), leaving the unbound target molecule behind in the clarified liquid [57].

Although the discrimination of some contaminants is challenging to achieve with conventional, low-cost adsorbents, improved selectivity can be attained by designing adsorbents with affinity ligands specific for certain impurities classes. On the other hand, the need to engineer the given specificity of adsorbents makes this process more expensive [47].

1.4.4.1. Solid-phase extraction (SPE)

SPE is a sample preparation technique in which preconcentration, extraction, and clear-up procedures are simultaneously performed to achieve fast and efficient purification without using volatile and hazardous organic solvents [58,59]. This extraction procedure allows the removal of contaminants from biological [60], environmental, clinical [61],

food, and beverage samples [62]. Other uses of SPE include storage of micro-pollutants from environmental samples [63], desalting proteins and sugar samples [64], derivatization [65], concentration of pigments, and changing solvents [66]. Besides, several SPE procedures are recommended as Environmental Protection Agency (EPA) methodologies [58].

SPE has played a crucial role in sample preparation in recent decades, replacing the traditional liquid-liquid extraction (LLE) [67]. The principle of SPE is similar to that of LLE, consisting of loading a solution onto a solid-phase capable of retaining the target analyte, washing away undesired components, or vice-versa [67–69]. As illustrated in Figure 4, the basic SPE procedure consists of four consecutive steps. First, the solid sorbent should be conditioned/equilibrated using an appropriate solvent (usually the same solvent as the sample) to enable the wetting of packing material and possible removal of impurities contained in the sorbent. The second step is the loading step, where the sample is injected, and the separation occurs. During this step, the analytes are concentrated on the sorbent, enabling some purification of the sample. In the third step, the solid-phase washing is done, employing an appropriate solvent with a low elution strength to eliminate matrix components that have been retained by the solid sorbent without displacing the analytes. The final step comprises the elution of the analytes of interest and the regeneration of the matrix by an appropriate solvent [58], [68].

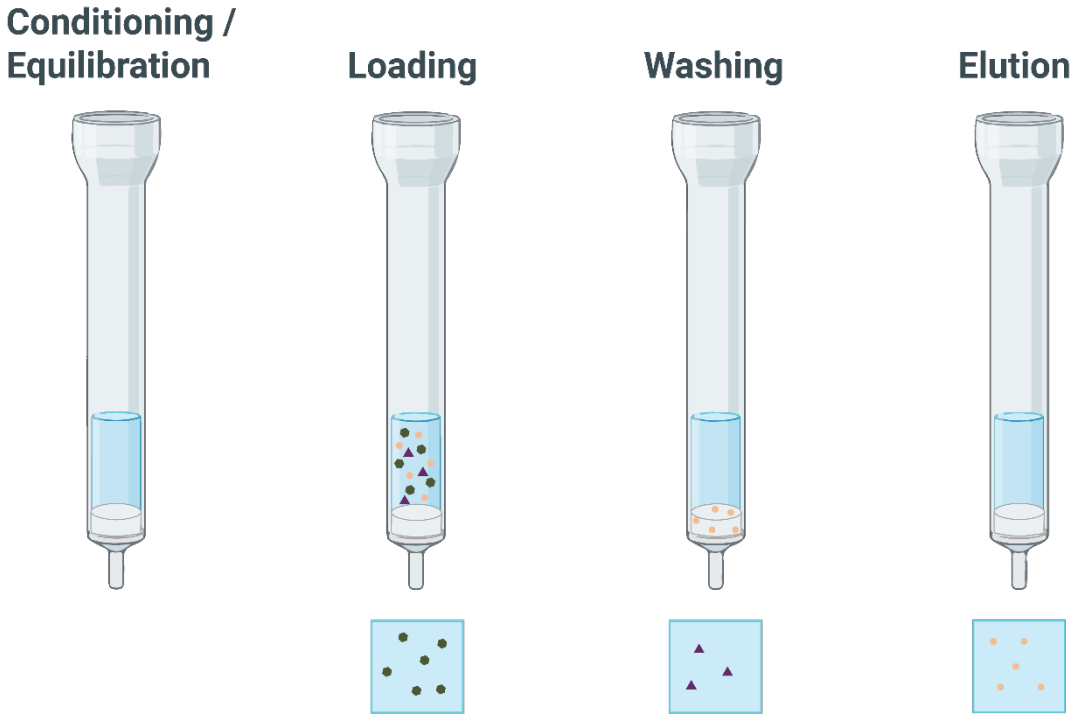

Figure 4 - Common SPE procedure, comprising conditioning, loading, washing, and elution.

Compared to LLE, SPE is faster and less labor-intensive while extracting a wide range of organic analytes from a large variety of samples, achieving high extraction efficiency and not forming emulsions. One other significant advantage is that the analytes adsorbed onto the solid-phase can be prevented from degradation and thus be stored for a certain period without any change in their concentration or identity [69]. The research group of Telepchak reported that SPE is more selective than LLE, although this statement is somehow controversial since other authors have pointed out that SPE suffers from a lack of selectivity [61]. SPE procedures often require several steps becoming cumbersome and time-consuming [69]. Thus, several materials have been designed to act as a sorbent, and some other sample-preparation methodologies such as solid-phase dynamic extraction (SPDE), micro-extraction by packed sorbent (MEPs), matrix solid-phase dispersion (MSPD), stir-bar sorptive extraction (SBSE), solid-phase micro-extraction (SPME), automated headspace dynamic solid-phase extraction, and dispersive solid-phase extraction (d-SPE) have been developed as new branches of SPE technique [58,67].

This last extraction procedure, d-SPE, has received much attention, and it is the method chosen to develop this work. The difference between this procedure and basic SPE is that sorbent is dispersed in the sample solution, and thus contact surface between the analyte and sorbent increases dramatically, resulting in increased extraction efficiency and reduced extraction time [70]. As shown in Figure 5, extraction of an analyte is achieved by adding a certain amount of sorbent particles to the sample. After adsorption, nanoparticles are collected via centrifugation or by an external magnet (when using magnetic particles). In the next step, extracted analytes are desorbed in a suitable solvent and then quantified using an appropriate analytical instrument.

Although SPE origins are as old as chromatography, this extraction method remains a dynamic field, with a flux of research far from concluded [70].

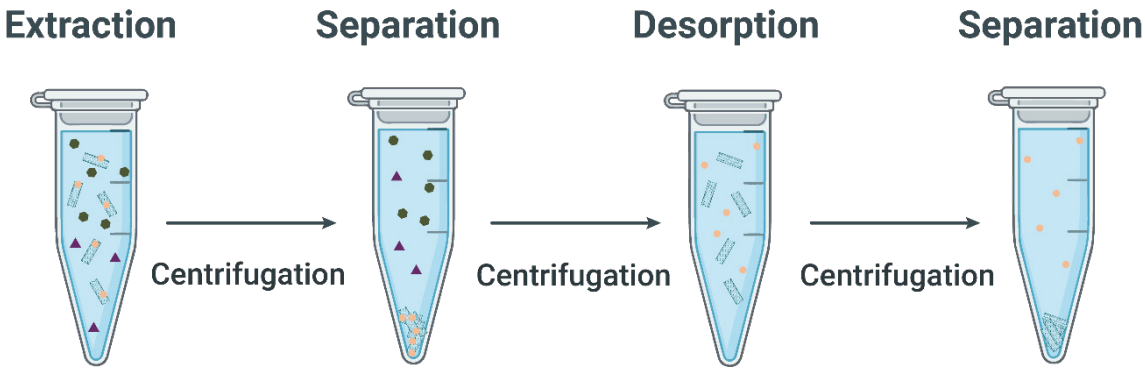

Figure 5 - Representation of d-SPE operation steps, including extraction, separation, desorption, and separation.

1.4.4.1.1. CNTs as adsorbents in SPE

CNTs have gained attention on SPE due to their remarkable structure and exceptional adsorption properties [71]. Because of these characteristics, CNTs are promising candidates for acting as adsorption material to remove or recover dyes, heavy metals, proteins, and nucleic acids [60]. To date, to separate and purify molecules, several steps have to be performed, like extraction, precipitation, concentration, and purification, among others. So, it becomes essential to focus on exploring efficient, accurate, sensitive, selective, and easy-to-operate sample purification techniques [59]. In all cases, the development of these SPE-CNTs undergoes a series of steps until it is optimized. Diverse factors affect the previous stages, like the type and quantity of CNTs used, the influence of pH, sample volume, buffer type, and concentration of the binding and elution solutions, among others [59].

Two types of nanotubes can be considered according to their use in SPE: as-grown (also known as pristine) and functionalized CNTs. As-grown nanotubes can be considered all CNTs that were obtained from synthesis and posterior purification. Because they are ready to use as sorbent, these are easy to use, although they also possess some disadvantages [59]. As-grown CNTs possess nonpolar bonds and high aspect-ratio and are thus insoluble in most organic solvents and aqueous solutions, resulting in a higher tendency to aggregate. Considering this, the use of these nanotubes impose some limitations [72]. Moreover, as-grown CNTs have inert walls with lack of functionalized groups, and the dominant interactions between pure CNTs and the molecules of interest are weak, mainly hydrophobic and π-π interactions, which make this type of CNTs to present low extraction capability and poor selectivity to diverse types of molecules [59]. Surface modifications can overcome these challenges.

As referred, functionalization of CNTs can occur by forming covalent bonds through chemical reactions with particular agents or forming noncovalent bonds through physical adsorption processes.

Table 4 summarizes all functionalization methods and the major advantages and disadvantages of the corresponding method. Although the chemical method can provide useful functional groups onto the CNT surface, this process has two drawbacks. Firstly, a functionalization reaction creates a large number of defects that can alter the properties of CNTs and, in some extreme cases, can fragment CNTs into smaller pieces. Secondly, the process is more complex and comprises several steps, and the use of strong acids and oxidants are not environmental friendly [73].

Table 4 - Chemical methods vs physical methods in CNTs functionalization

Method		Principle	Damage to CNTs	Easy to use
Chemical method	Sidewall	Hybridization of C atoms from sp2 to sp3	√	×
	Defect	Defect transformation	√	√
Physical method	Polymer wrapping	van der Waals forces, π–π stacking	×	√
	Surfactant adsorption	Physical adsorption	×	√
	Endohedral method	Capillary effect	×	×

An alternative is the use of noncovalent functionalization. The tunning of CNT surface can be achieved by polymer wrapping with polystyrene [74]; by employing surfactants to enhance dispersibility and other properties of CNTs, using for example polyoxyethylene octylphenylether (Triton X-100) [75]; or by endohedral method, for example, by the insertion of inorganic nanoparticles like, C_{60}, Ag, Au, and Pt into the tubes [76].

The type of strategy used is intrinsically related to the analyte to be recovered and the sample matrix in which the analyte is solubilized. Nevertheless, the state of the art indicates that functionalization (both by chemical and physical strategies) seems to be the future of this approach, since it allows the attachment of functional groups with directed selectivity for some specific molecules [59].

1.5. Gene therapy

Gene therapy has long been fascinating scientists, clinicians, and the general public for its potential to treat and prevent a wide range of diseases. Over the past two decades, the clinical applications of gene-based therapy have been investigated for the treatment of pathologies such as cardiovascular and neurodegenerative diseases, osteoporosis, and cancer [77,78].

Gene therapy is characterized by the intentional modulation of gene expression in specific cells to correct disease-causing mutations. This modulation is performed by inserting exogenous nucleic acids such as plasmid DNA (pDNA), messenger RNA (mRNA), small interfering RNA (siRNA), microRNA (miRNA), or antisense oligonucleotides [77,79]. However, as simple as the concepts sound, numerous barriers have to be overcome, from the development of safe and effective delivery vectors to improved stability and reduced immunogenicity of nucleic acids, numerous barriers and challenges have to be surpassed [78].

1.5.1. Strategies of gene therapy

Currently, two general strategies can be used in gene therapy: *ex vivo* and *in vivo* approaches (Fig. 6) [80]. In the *ex vivo* approach, patient's somatic cells are therapeutically modified outside the body in a laboratory and restored to the patient. The main advantage of *ex vivo* gene therapy includes specificity, safety, and lack of immune response. Also, in the *ex vivo* procedure, it is possible to select and analyze the modified cells [77,80,81]. In the strategy named *in vivo*, the nucleic acid is administered directly into the patient bloodstream or introduced directly into a localized area to target specific tissue. *In vivo* approaches have a significant advantage over *ex vivo*, since it avoids the cumbersome and costly process of removing cells from the patient, manipulating the cells *in vitro*, and returning the genetically modified cells to the patient [77,80].

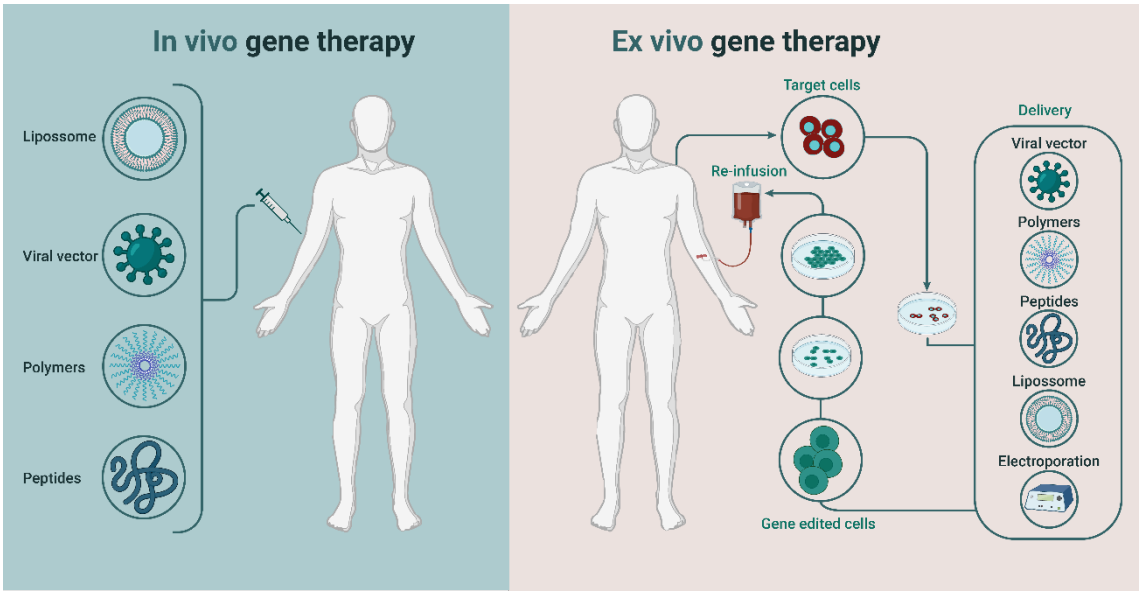

Figure 6 - Representation of *ex vivo* and *in vivo* approaches in gene therapy.

Independent of the overall strategy, to improve the efficiency and specificity of the gene transfer, a vector has to be chosen. An expression cassette package will be inserted into this viral or non-viral vector containing the genetic sequences to be delivered [80]. Although ~70% of gene therapy clinical trials carried out so far have used modified viruses such as retroviruses, lentiviruses, adenoviruses, and adeno-associated viruses (AAVs), several limitations are associated with viral vectors, including carcinogenesis, immunogenicity, broad tropism, limited DNA packaging capacity and difficulty of vector production [82]. Thus, non-viral gene therapy arises with the potential to control many of these limitations, particularly concerning safety. For instance, synthetic 'vehicles' tend to have lower immunogenicity than viral vectors, and patients do not have pre-existing immunity, as is the case with some viral systems. Non-viral vectors also can deliver larger genetic payloads and are typically easier to synthesize than viral vectors [82].

Together, the choice of vector, the design of the expression cassette, and the coding sequences of the gene determine the resulting gene expression.

1.5.2. Nucleic acid-based therapy

Since the world first approved gene therapeutic Gendicine, nucleic acids-based therapies have had a major impact on the pharmaceutical industry [79]. Over the last years, a series of pivotal discoveries have made this possible, from the decoding of the human genome that unlocked several critical molecular pathways, to the discovery and understanding of several RNA types with complex functions. Today, more than 2,000 clinical trials of nucleic acid therapies are underway [83].

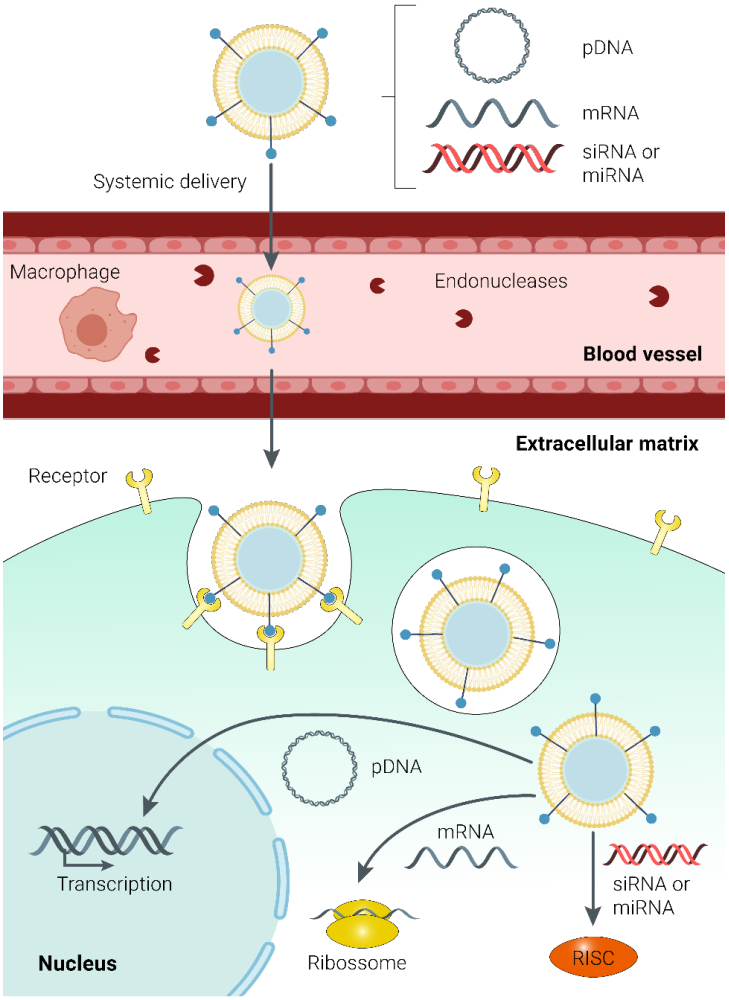

Figure 7 - *In vivo* delivery of nucleic acids using non-viral vectors.

1.5.2.1. DNA-based therapies

Plasmid DNA is highly negatively charged, a double-stranded DNA molecule composed of genes of interest and can be used to express mRNA or proteins for gene therapy. The success of the medicinal use of genes depends, first, on the efficiency of pDNA delivery method used and the expression of the administered gene in the target cells. To reach target cells, DNA has to overcome a series of defense barriers and mechanisms that act together to clear exogenous DNA molecules [84] (Fig.7).

1.5.2.2. mRNA-based therapies

mRNA has been studied as a potential alternative to DNA-based gene therapy for expression of therapeutic proteins in vivo. Although less stable, mRNA has less immunogenicity, does not require nuclear localization for expression, and no potential mutagenesis occurs from genomic integration [82].

1.5.2.3. RNAi-based therapies

RNAi involves the pairing of a short RNA sequence with endogenous mRNA target, leading to highly specific degradation, and can regulate gene expression through a post-transcriptional gene silencing mechanism. The constituent members of RNAi therapeutics mainly include siRNA and miRNA. siRNA have a great therapeutic potential since has the ability to silence nearly any targeted gene after introduction into cells. miRNAs are endogenously synthesized and promote mRNA degradation and translational inhibition [80,82].

1.5.3. Challenges of pDNA downstream processing

Several unit operations have to be arranged to purify plasmid biopharmaceuticals, with the primary goal of removing impurities associated with the recombinant organism used for production, in order to reach the acceptable quality, considering the therapeutic application purposed. For numerous reasons, this process undertakes several challenges, mostly due to the diversity of solutes derived from the producer organism (usually *E. coli*) [85]. Since most *E. coli*-derived impurities share several properties with pDNA, it is expected that these impurities behave, to some extent, in a similar way to the plasmid. For example, RNA and gDNA molecules have identical charge to pDNA, and the molecular weight of gDNA and pDNA may also be comparable. These similarities can compromise the selectivity of operations that attempt to explore charge and size differences for separation purposes [86]. Hence, plasmids and *E. coli* impurities are likely to compete and copurify with each other. One solution to these problems is to focus on properties that differ between plasmids and impurities, like hydrophobicity. The differences found here are intimately linked to the fact that plasmids are essentially double-stranded, while RNA and fragmented gDNA are, for the most part, single-stranded or are present in a denatured form. This offers the possibility to explore interactions with and between exposed bases for separation purposes, expecting to achieve a significant reduction of impurities [47]. By exploring these molecular differences and combining them with MWCNTs powerful adsorption capacity, this study proposes a method for the capture and pre-purification of nucleic acids, establishing a technology that can highly support and facilitate the final purification of plasmid DNA.

CHAPTER 2

2. Objectives

The primary purpose of this study is to develop a simple and efficient method for the pre-purification of plasmid DNA from *E. coli* lysate sample based on the unique adsorptive properties of as-grown MWCNTs. Herein, selectivity between different nucleic acid species is intended. For that, the structural differences between impurities, like RNA and gDNA, and pDNA will be explored, such as the exposure of RNA and gDNA bases that, in theory, will interact more with MWCNTs surface, displaying more affinity towards carbon nanotubes than pDNA.

To achieve an effective isolation method, a series of tasks were designed:

1. Evaluate different MWCNTs diameters to study the best adsorption strategy. It is also intended to develop an effective strategy to elute and regenerate MWCNTs for the MWCNTs reuse.
2. Study the affinity and selectivity of MWCNTs towards pDNA and RNA.
3. Control the reduction of impurities in the sample after MWCNTs extraction, to assess the method performance.
4. Assess pDNA stability after isolation, and perform additional cytotoxicity of MWCNTs, to evaluate their safety.
5. Develop a simple, rapid, and more eco-friendly way to isolate pDNA for further purification.

CHAPTER 3

3.Materials and Methods

3.1. Materials

For dispersive solid-phase extraction of nucleic acids, different MWCNTs were kindly provided by Doctor Cláudia Gomes Silva (Faculty of Engineering of the University of Porto). MWCNTs properties are further described in Table 5. The reagents used in the different adsorption experiments were ammonium sulfate ($(NH_4)_2SO_4$), Tween-20 ($C_{58}H_{114}O_{26}$), sodium hydroxide (NaOH), sodium dodecyl sulfate (SDS), sodium chloride (NaCl) commercialized by Panreac (Barcelona, Spain), and tris(hydroxymethyl)aminomethane (Tris) from Merck (Darmstadt, Germany).

Table 5 - General MWCNTs characteristics.

Model	OD	Length	Purity	ASH	SSA
MWCNT- <10	7-15nm	>5µm	>97%	<3 wt%	250~500m²/g
MWCNT-<10/20	10-20nm	>5µm	>97%	<3 wt%	100~160m²/g
MWCNT-20/40	20-40nm	>5µm	>97%	<3 wt%	80~140m²/g
MWCNT-60/100	60-100nm	>5µm	>97%	<3 wt%	40~70m²/g

(OD – Outer diameter; SSA – Specific surface area; ASH – ash content.)

For *E. coli* DH5α bacteria growth, the reagents used were "Luria-Bertani" (LB) agar from Pronalab (Mérida, Mexico), tryptone and yeast extract from Bioakar (Beauvais, France), glycerol from Himedia, dipotassium hydrogen phosphate (K_2HPO_4) from Panreac (Barcelona, Spain), potassium dihydrogen phosphate (KH_2PO_4) from Sigma-Aldrich (St. Louis, Missouri, EUA) and kanamycin antibiotic from Thermo Fisher Scientific Inc. (Waltham, EUA).

For nucleic acids extraction, the reagents used were guanidine thiocyanate, N-Lauroylsarcosine sodium salt, sodium citrate, and isoamyl alcohol, from Sigma-Aldrich (St. Louis, Missouri, USA), isopropanol from Thermo Fisher Scientific Inc. (Waltham, USA), and β-mercaptoethanol from Merck (Whitehouse Station, USA). For plasmid DNA extraction, the NZYMaxiprep kit from NZYTech Genes and Enzymes (Lisbon, Portugal) was used. For alkaline cell lysis it was used solution A comprising Tris from Merck (Darmstadt, Germany) and EDTA from Sigma-Aldrich (St. Louis, Missouri, USA);

solution B with NaOH and SDS from Panreac (Barcelona, Spain); and solution C with potassium acetate from Panreac (Barcelona, Spain). For nucleic acids visualization in electrophoresis, Green-Safe reagent was used from Grisp (Porto, Portugal).

Dye Reagent Concentrate and bovine serum albumin (BSA), both from Bio-Rad (California, EUA), were used for protein quantification. For real-time quantitative PCR (qPCR) assays, Maxima® SYBR Green/Fluorescein qPCR Master Mix Kit from Thermo Fisher Scientific Inc. (Waltham, EUA) was used. The primers for these experiments were 5'ACACGGTCCAGAACTCCTACG-3′ (forward) and 5′-CCGGTGCTTCTTCTGCGGGTAACGTCA-3′ (reverse), from Stabvida (Caparica, Portugal). The pDNA quantification was carried out by analytical chromatography, using a CIMac™ pDNA 0.3 mL analytical column from Bia Separations (Slovenia).

For human dermal fibroblasts (hFIB) culture it was used the "Dulbecco's Modified Eagle's Medium/Nutrient Mixture F-12" (DMEM-F12) from Sigma-Aldrich (St. Louis, Missouri, USA), fetal bovine serum (FBS) from Gibco, Life Technologies (EUA), and penicillin-streptomycin from Grisp (Porto, Portugal). The cytotoxicity assay was performed with the Cell Proliferation Kit I (MTT) from Merck (Darmstadt, Germany).

All solutions were prepared with Ultrapure reagent-grade water, purified with a Milli-Q system from Millipore (Billerica, MA, USA).

3.2. Methods

3.2.1. *E. coli* growth and nucleic acids production

RNA and pDNA used in this study were obtained from a culture of *E. coli* DH5α strain, previously transformed with the plasmid pBHSR1-RM containing the human sequence of pre-miR-29b. For the assays where cell lysate was required, *E. coli* DH5α strain with 6.07-kb pcDNA3-FLAG-p53 Addgene plasmid 10838 containing human sequence of p53 was used. Initially, *E. coli* was inoculated in LB-agar medium supplemented with 50 μg/mL of kanamycin, and the growth occurred at 37 ºC overnight. Pre-fermentation was carried out by transferring some colonies to shake flasks containing 125 mL of Terrific Broth medium (12 g/L tryptone, 24 g/L yeast extract, 4 mL/L glycerol, 0.017 M KH_2PO_4, 0.072 M K_2HPO_4), supplemented with kanamycin 50 μg/mL. The *E. coli* growth occurred at 37 ºC, 250 rpm, until an optical density at 600 nm (OD_{600}) of around 2.6 was achieved. The following equation was used to calculate the pre-fermentation volume needed to start fermentation at an OD_{600} of 0.2:

$$V_{\text{from pre-fermentation}} = (V_{\text{pre-fermentation}} + V_{\text{fermentation}}) \times OD_{\text{fermentation}}/OD_{\text{pre-fermentation}}$$

To measure the OD, a spectrophotometer Pharmacia Biotech Ultraspec 3000 UV/Visible (Cambridge, England) was used. Bacterial growth was kept for 8 h or 16 h, if RNA (with low molecular weight) or pDNA, were required. Cells were recovered by centrifugation at 3900 g for 10 minutes at 4 ºC, being the pellets stored at -20 ºC.

3.2.2. Plasmid DNA extraction

For the recovery and extraction of pDNA, NZYMaxiprep kit was used, according to the protocol provided by the manufacturer. Briefly, the bacterial pellet corresponding to 100 mL of *E. coli* culture was resuspended in 12 mL of Buffer M1, containing RNase A, by vigorous vortexing. As pDNA is an intracellular product, cell lysis had to be performed. Hence, 12 mL of Buffer M2 was added, and homogenization was performed by gently mix by inverting the tube. After 5 minutes of incubation at room temperature, the neutralization step was carried out by adding 12 mL of pre-cooled Buffer M3, and the bacterial suspension was carefully homogenized. The lysate was then centrifuged for 30 min at 20,000*g* at 4 °C. If the supernatant still contained suspended matter, centrifugation was repeated for 15 min. Meanwhile, the NZYTech column was equilibrated with 6 mL of Buffer MEQ. After centrifugation, the supernatant was transferred to the equilibrated NZYTech column. In this step, DNA binding occurred, and the contaminants are eliminated by washing the column with 32 mL of Buffer MW. For the elution of pure pDNA, 15 mL of Buffer ME was added and pDNA was recovered into new tubes. Eluted pDNA was then precipitated with 10.5 mL of isopropanol, followed by careful homogenization and 15 minutes of incubation on ice. Then, a centrifugation was performed at 15,000*g* for 30 minutes, at 4 °C. The supernatant was discarded, and DNA pellet was washed with 5 mL of 70% ethanol. The centrifugation was repeated at 15,000*g* for 15 minutes, at 4 °C. Carefully, ethanol was removed entirely, and the pellet was left to dry at room temperature. For DNA reconstitution, the DNA pellet was dissolved in 1 mL of Buffer TE (10 mM Tris-HCl and 1 mM EDTA pH 8.0). The final pDNA sample was quantified using a NanoPhotometer (IMPLEN, United Kingdom). The integrity and purity of the sample were evaluated by agarose gel electrophoresis and at the end, the DNA samples were stored at -80˚C.

3.2.3. Low molecular weight RNA extraction

RNA extraction and isolation were performed by the method of acid guanidinium thiocyanate-phenol-chloroform. After thawing the *E. coli* cells pellet, a solution of 0.8 %

NaCl was used for resuspension, followed by centrifugation at 6000*g*, for 10 minutes, at 4 ºC. The supernatant was discarded, and the resultant pellets were resuspended with 5 mL of solution D (4 M guanidinium thiocyanate, 0.025 M sodium citrate pH 7, 0.5 % sodium N-lauroylsarcosinate, and 0.1 M β-mercaptoethanol) and incubated in ice for 10 minutes. At this point, fragmentation of DNA occurs, minimizing its presence in the aqueous phase. After, 0.5 mL of 2 M sodium acetate pH 4 and 5 mL of phenol were added to the suspensions, being carefully homogenized at each step. Then, 1 mL of a mix of chloroform/isoamyl alcohol (49:1) was added, followed by vigorous shaking and incubation in ice for 15 minutes. The suspensions were centrifuged at 10000*g* for 20 minutes, at 4 ºC. Extraction is achieved at this stage, and two aqueous phases are formed, being the upper phase enriched in RNA while the bottom phase is enriched in DNA. So, the upper phase must be very carefully transferred to new tubes, avoiding DNA contamination. 5 mL of isopropanol was added to the aqueous phase, and RNA samples were incubated in ice to promote RNA precipitation. Centrifugation was then accomplished at 10000*g* for 20 minutes at 4 ºC. After discarding the supernatant, a second precipitation is done. RNA pellets were dissolved in 1.5 mL of solution D, and then 1.5 mL of isopropanol, followed by centrifugation at 10000*g* for 10 minutes at 4 ºC. The supernatant was discarded, and resultant pellets were washed through resuspension in 2.5 mL of 75% ethanol in DEPC water, followed by incubation of the samples at room temperature for 10-15 minutes to dissolve possible residual traces of guanidinium. Centrifugation at 10000*g* for 5 minutes at 4 ºC was performed, and the resulting pellet was dried for 5-10 minutes at room temperature. Finally, RNA pellets were dissolved in 1 mL of DEPC treated water and incubated at room temperature for 10-15 minutes to complete solubilization. The concentration of RNA was measured in the Nano Photometer (IMPLEN, United Kingdom), and the integrity of the samples was verified by agarose gel electrophoresis, being the samples stored at -80 ˚C until use.

3.2.4.Total Nucleic acids extraction

For initial screening assays with both RNA and pDNA, nucleic acids extracts from *E. coli* cells were used. Pellets were resuspended in 5 mL of solution D, dissolving the cellular membrane. The lysis tubes were then incubated in ice for 10 minutes, followed by centrifugation at 16000*g* for 30 minutes at 4 ºC. To precipitate nucleic acids, 5 mL of isopropanol was added to the supernatant. The tubes were then incubated in ice for 30 minutes and then centrifuged at 16000*g* for 20 minutes at 4 ºC. After discarding the supernatant, the pellet was washed and dried by adding 2.5 mL of 75 % ethanol-DEPC to each tube, followed by room temperature incubation for 10 minutes. Centrifugation at

16000*g* for 5 minutes at 4 ºC was performed, the supernatant was discarded, and pellets were air-dried for 10 minutes. Pellets were dissolved in 2 mL of DEPC treated water and incubated in a 60 ˚C water bath for 10 minutes and finally centrifuged at 16000*g* for 30 minutes at 4 ºC, being the supernatant recovered. The concentration of nucleic acids was measured in the Nano Photometer (IMPLEN, United Kingdom), and the integrity of the samples was verified by agarose gel electrophoresis, being the samples stored at -80 ºC.

3.2.5. Cell lysate extraction

A modified alkaline lysis method was used to perform cell lysis and recover a lysate sample containing a complex matrix comprising, pDNA, gDNA, RNA and proteins. Thus, *E. coli* cells pellet was resuspended in 10 mL of solution A (50 mM Tris-HCl, and 10 mM EDTA at pH 8.0) followed by the addition of 5 mL of solution B (200 mM NaOH and 1% (w/v) SDS). Then, samples were incubated for 5 minutes at room temperature to promote cell lysis. To neutralize the samples, 5 mL of solution C (3 M potassium acetate at pH 5.0) was added, followed by incubation on ice for 20 minutes. After, the tubes were centrifuged twice at 20 000*g* for 30 minutes at 4 ºC to eliminate significant cell debris, some gDNA, and proteins, the supernatant was stored at -80 ºC until further use.

3.2.6. Dispersive solid-phase extraction of RNA using MWCNTs

D-SPE was mainly applied to capture RNA from complex *E. coli* lysates using as-grown MWCNTs. Several strategies had to be optimized until an efficient method was discovered. Figure 8 represents the full process developed in this work.

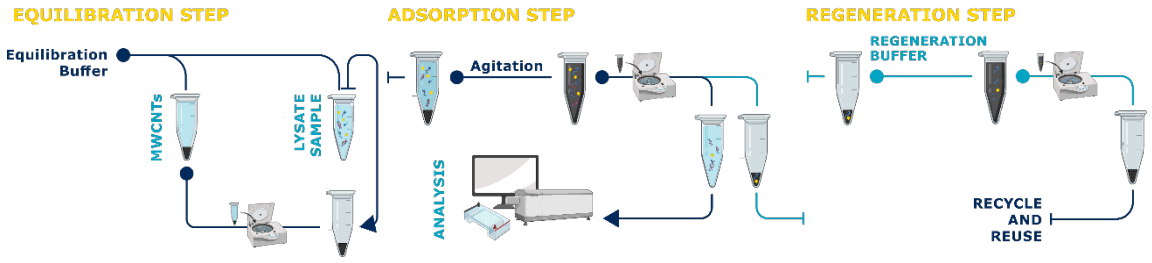

Figure 8 - Schematic of d-SPE procedure.

This method comprises three main steps:

- The equilibration step, where 1 mg of as-grown MWCNTs were equilibrated using an appropriated equilibration buffer. The equilibration step was followed by 20

minutes of agitation and posterior centrifugation at 8000*g* for 2 minutes to remove the aqueous phase. Also, the sample to be extracted was diluted with the same equilibration buffer.

- The adsorption step, where the sample to be extracted was applied in the MWCNTs. The mixture was kept at room temperature, in agitation, for 20 minutes to allow nucleic acid adsorption onto MWCNTs. Then, another centrifugation at 8000*g* for 2 minutes was performed to separate the solid-phase from the aqueous phase (supernatant). The supernatant was stored for further analysis, namely for measuring the absorbance in the Nano Photometer (IMPLEN, United Kingdom) and run an agarose gel electrophoresis. This analysis allowed the evaluation of the adsorption behavior.
- The regeneration step, where a regeneration buffer was applied to solid-phase MWCNTs to remove the remaining bound species. This mixture was agitated for 20 minutes and then centrifugated at 8000*g* for 2 minutes to remove the aqueous phase. To ensure the total removal of regeneration buffer, three washes were performed on the MWCNTs with deionized water. Finally, MWCNTs were air-dried for 24 hours and stored for further use.

Different sample composition and buffers were used in the course of this work. Their composition and purpose are explained in the "Results" section.

3.2.7. Agarose gel electrophoresis

Nucleic acids analysis, regarding the evaluation of the identity and relative purity of different samples was continuously performed by agarose gel electrophoresis in 1 % agarose gel. Nucleic acids were stained in the gel with 0.012 µL/mL of Green Safe, and electrophoresis was run at 120 V for 30 minutes in TAE buffer (40 mM Tris base, 20 mM acetic acid, and 1 mM EDTA, pH 8.0). The gels were visualized under ultraviolet (UV) light exposure in the Uvitec Cambridge with a UV chamber (UVITEC Cambridge, Cambridge, United Kingdom).

3.2.8. Circular Dichroism spectroscopy

Circular Dichroism (CD) experiments were performed to assess the stability of pDNA after the extraction procedure. CD was done in a Jasco J-815 spectropolarimeter (Jasco, Easton, MD, USA), using a Peltier-type temperature control system. CD spectra were acquired at a constant temperature of 20 °C using a scanning speed of 50 nm/min, with a response time of 1 second over wavelengths ranging from 210 to 320 nm. The recording

bandwidth was 1 nm with a step size of 1 nm using a quartz cell with an optical path length of 1 mm. Three scans were measured per spectrum to improve the signal-to-noise ratio, and the spectra were smoothed using the smooth tool in OriginPro 2018 software.

3.2.9. Plasmid DNA assessment

The purity and recovery of pDNA were evaluated using a CIMac™ pDNA 0.3 mL analytical column. First, it was performed a calibration curve using as standard a p53-encoding pDNA, previously isolated and purified with the NZYMaxiprep kit from *E. coli*. Different standards with concentrations ranging from 5 to 150 µg/mL were prepared and injected onto the monolithic column, to determine the calibration curve, as shown in Figure 9.

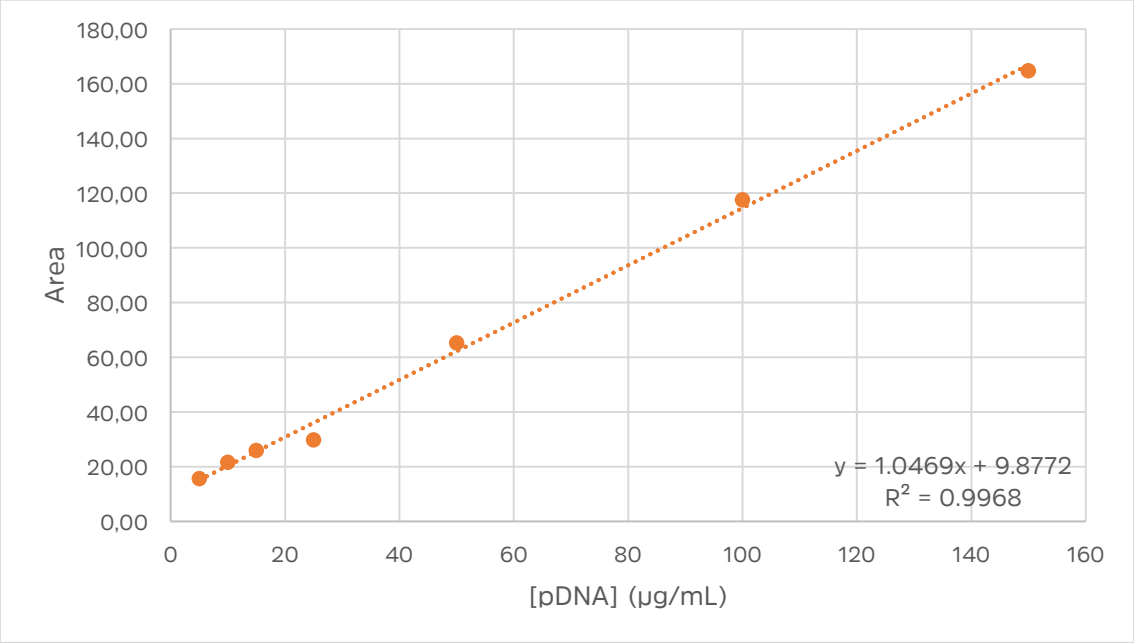

Figure 9 - Calibration curve obtained from the injection of pDNA standards with concentrations in the range of 5 to 150 g/mL.

For the chromatographic experiments, the analytical column was first equilibrated with 95 % of 0.5 M NaCl in 100 mM Tris-HCl pH 8.0 and 5% of 1 M NaCl in 100 mM Tris-HCl pH 8.0. Subsequently, pDNA samples were injected, and it was applied a step gradient of 1 M NaCl in 100 mM Tris-HCl pH 8.0 after 3 minutes. After sample elution, a washing step was added by applying 95 % of 0.5 M NaCl in 100 mM Tris-HCl pH 8.0 and 5% of 1 M NaCl in 100 mM Tris-HCl pH 8.0 for 3 minutes. Regeneration of the column was performed by adding 2 M NaCl in 100 mM Tris-HCl pH 8.0 for 2 minutes to remove

bound substances from the stationary phase, and it was followed by re-equilibration of the column with the appropriated counter-ion by applying 95 % of 0.5 M NaCl in 100 mM Tris-HCl pH 8.0 and 5% of 1 M NaCl in 100 mM Tris-HCl pH 8.0 for 6 minutes. The chromatogram peaks in Figure 10 were integrated, allowing a correlation between peak area and pDNA concentration. All samples were analyzed in triplicate, and the peak area was averaged from those values.

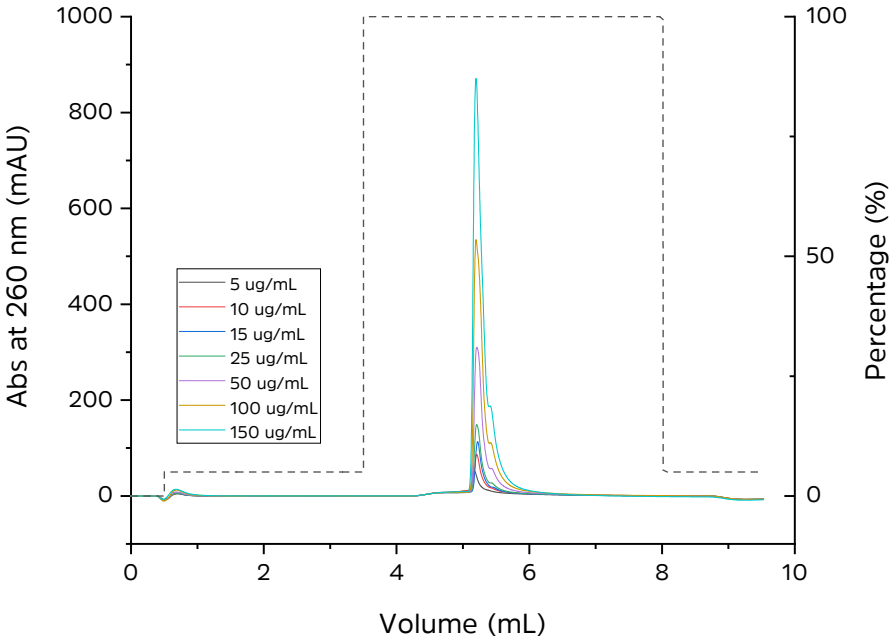

Figure 10 - Chromatographic profile of pDNA at different concentrations.

3.2.10. Plasmid DNA quality control

3.2.10.1. Total protein quantification

Bradford Protein Assay was used to determine the total protein concentration present in the pDNA samples. Firstly, a calibration curve was designed, using BSA as standard protein, in the linear range from 0.05 to 0.5 mg/mL. Then, Dye Reagent Concentrate preparation was done by diluting 1 part of dye reagent and 4 parts of distilled, deionized water, followed by filtration to remove particulate material. Each standard and sample solution were quantified in triplicate using 10 µL of sample and 200 µL of Dye Reagent Concentrate. The absorbance of the plate was evaluated at 595 nm, and the amount of protein was calculated using the calibration curve represented in Figure 11.

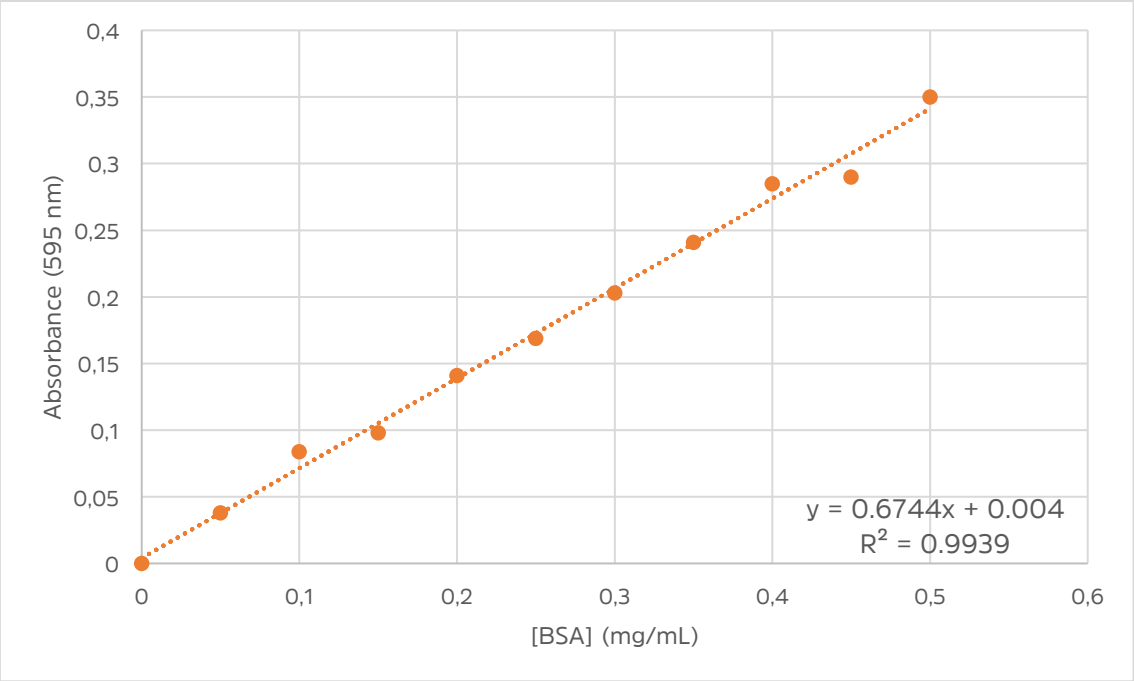

Figure 11 - Calibration curve obtained from BSA standards with a range of concentrations from 0.05 to 0.5 mg/mL.

3.2.10.2. Genomic DNA quantification

For quantitative analysis of gDNA present in the sample, qPCR was performed in 96-well optical plates, using the Maxima® SYBR Green/Fluorescein qPCR Master Mix (2X) (Thermo Fisher Scientific Inc.) in a CFX Connect™ Real-Time PCR Detection System (BioRad). To quantify gDNA, a calibration curve was designed with gDNA concentrations varying from 0.005 to 50 ng/µL. The calibration curve was obtained by a correlation between the quantitation cycle (Cq) and the logarithmic of gDNA concentration (Figure 12).

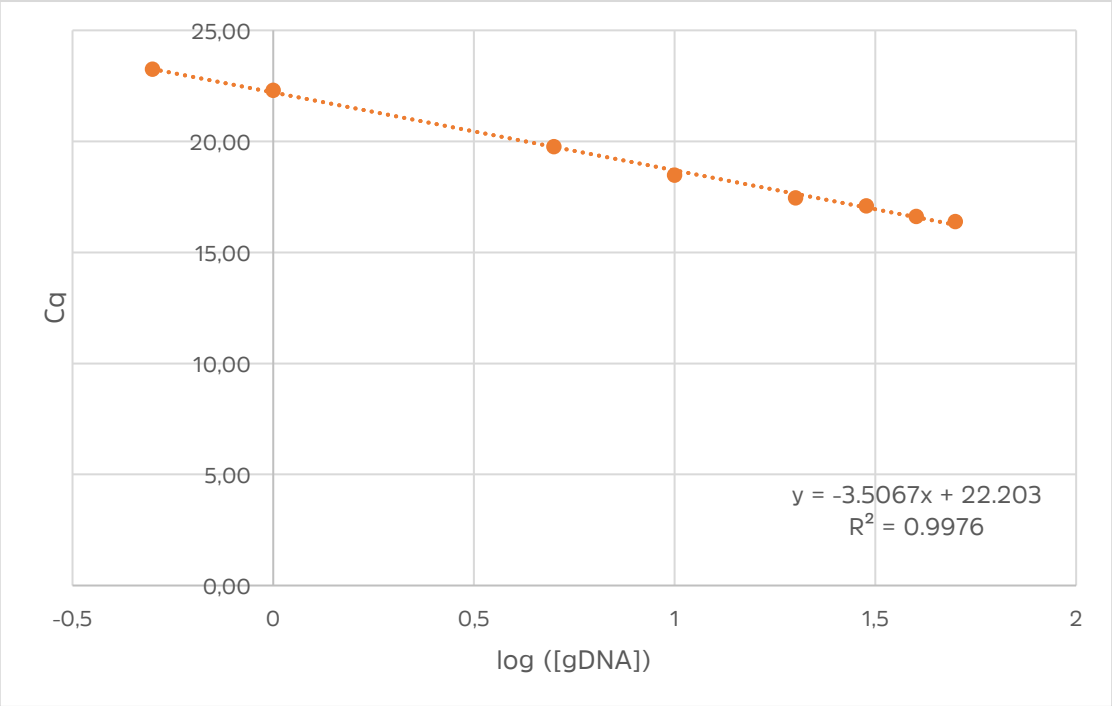

Figure 12 - Calibration curve obtained from gDNA standards with a range of concentrations from 0.005 to 50 ng/uL.

qPCR reaction was prepared to contain: 1 µL of the sample, 1.2 µL each specific primer (forward primer - 5'ACACGGTCCAGAACTCCTACG-3'; and reverse primer - 5'-CCGGTGCTTCTTCTGCGGGTAACGTCA-3') were used to amplify a 181-bp fragment of the 16S rRNA gene, 10 µL of Maxima® SYBR Green/Fluorescein qPCR Master Mix (2X) and 6.6 µl of nuclease-free water, to a final volume of 20 µL per reaction. The reaction conditions were 95 ˚C for 10 min for initial denaturation, followed by 39 cycles of 95 ˚C for 10 sec, 60 ˚C for 30 sec, and 72 ˚C for 15 sec. In the end, the samples were incubated at 65 ˚C for 5 sec with an increment of 0.5 ˚C until 95 ˚C for the melting curves. All reactions were completed in triplicate, and Cq values were averaged from the triplicate.

3.2.11. hFIB cell culture and cytotoxicity assay (MTT)

Normal human dermal fibroblasts (hFIB) were used for the cytotoxicity evaluation of MWCNTs. Cells were cultured in DMEM-F12 medium (Sigma-Aldrich) supplemented with 10 % (w/v) FBS heat-inactivated and 1 % (w/v) penicillin-streptomycin. Cell Proliferation Kit I (MTT) assay was used to assess cytotoxicity effects of different concentrations of as-grown <10 MWCNTs. hFIB cells at passages 10-20 were scattered at a density of $1x10^4$ cells per well in a 96-well plate, and after 24 h the cell culture medium was replaced by a new medium. Then, 25 µg, 50 µg, and 100 µg of MWCNTs

were placed in each well. MTT was also performed at different time points, namely 24 and 48 h. So, after the incubation period, the medium was replaced by 100 µL of new medium, and 10 µL of MTT labeling reagent was added. Cells were then incubated for 4 hours at 37 ˚C in a humidified atmosphere containing 5 % CO_2. Following incubation, the medium was removed, and 100 µL of dimethyl sulfoxide (DMSO) was added to each well to dissolve MTT crystals, and the plate was placed in agitation for about 15 minutes. The absorbance measurements were performed in a microplate reader at 570 nm. All experiments were repeated in triplicate, and for positive control for cytotoxicity, cells were treated with 70 % ethanol.

3.2.12. Statistical analysis

All cytotoxicity experiments were repeated three times using independent culture preparations. The data are expressed as mean ± standard error. Quantitative data were statistically analyzed by One-Way Analysis of Variance (ANOVA), followed by Turkey's multiple comparison test. "*" indicates a significant difference versus untreated cells.

CHAPTER 4

4. Results and Discussion

4.1. Screening of adsorption conditions

Since the first aim for this dissertation was to capture RNA from *E. coli* lysates using MWCNTs, it was necessary to explore the best conditions for the capture strategy. Hence, it was designed a series of screening assays, in which was studied the vital conditions for adsorption and desorption of RNA. First, different MWCNTs diameters were tested, and the conditions to exploit different interactions between MWCNTs and RNA were also addressed. The promotion of both electrostatic and hydrophobic interactions and the evaluation of different MWCNTs allowed observe the influence that these parameters have in RNA capture and adsorption.

Aliquots containing 1 mg of as-grown MWCNTs were prepared and equilibrated with the appropriate buffer. When the promotion of electrostatic interactions was desired, the equilibration stage was performed by applying 1 mL of 10 mM Tris-HCl pH 8 to MWCNTs. On the other hand, when it was to establish hydrophobic interactions, 1 mL of 1.5 M $(NH_4)_2SO_4$ in 10 mM Tris-HCl pH 8 was applied to MWCNTs. The equilibration step was followed by 20 minutes of agitation and posterior centrifugation at 8000*g* for 2 minutes, to recover equilibrated MWCNTs. A previously prepared low molecular weight RNA (50 μg/mL) sample, diluted in equilibration buffer, was added to MWCNTs in the binding step. The mixture was kept at room temperature, in agitation, for 20 minutes to allow nucleic acid adsorption onto MWCNTs. Then, the solid-phase was separated from the aqueous phase and the absorbance of the aqueous phase was then measured to quantify RNA not adsorbed to MWCNTs. This was repeated for the MWCNTs with different diameters to compare the adsorption performance of each one and study the influence of different conditions on the interaction and adsorption of RNA.

Four types of MWCNTs were applied to extract RNA, promoting both electrostatic and hydrophobic interactions in these initial experiments. As depicted in Figure 13, when promoting electrostatic interactions, low RNA adsorption was achieved, for all MWCNTs diameters. This phenomenon is because the MWCNTs surface is inert; hence, electrostatic interactions between the RNA and MWCNTs surface are unattainable.

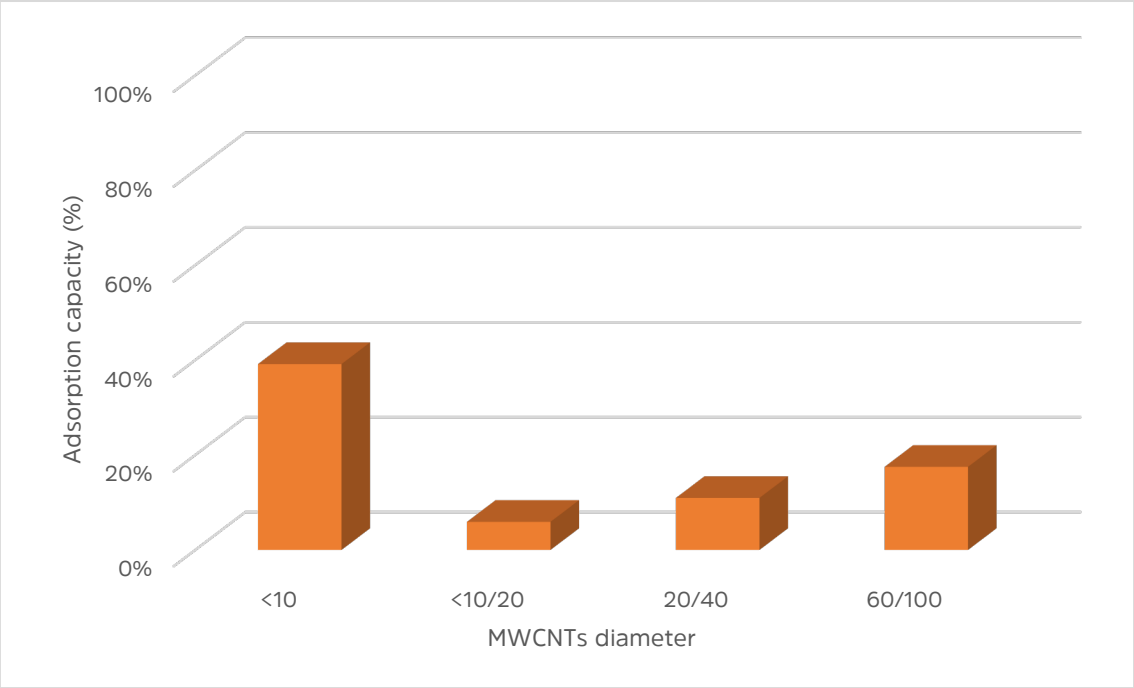

Figure 13 - RNA adsorption onto MWCNTs with different diameters, when promoting electrostatic interactions.

On the other hand, as shown in Figure 14, high RNA adsorption was achieved when establishing conditions that mainly promote hydrophobic interactions. The results also indicate that the adsorption capacity is higher in MWCNTs with smaller diameters. When comparing the adsorption percentage, it is possible to observe a significant increase from 69% obtained with <10/20 MWCNTs to 94% of adsorption capacity of <10 MWCNTs. This was expected since smaller diameter results in a higher surface area. Moreover, when comparing these adsorption percentages with the values of specific surface area (SSA) (Table 5) for each MWCNT, it is possible to see a clear correlation, since <10/20 MWCNTs have a lower SSA of 100~160 m^2/g in comparison with 250~500 m^2/g of <10 MWCNTs.

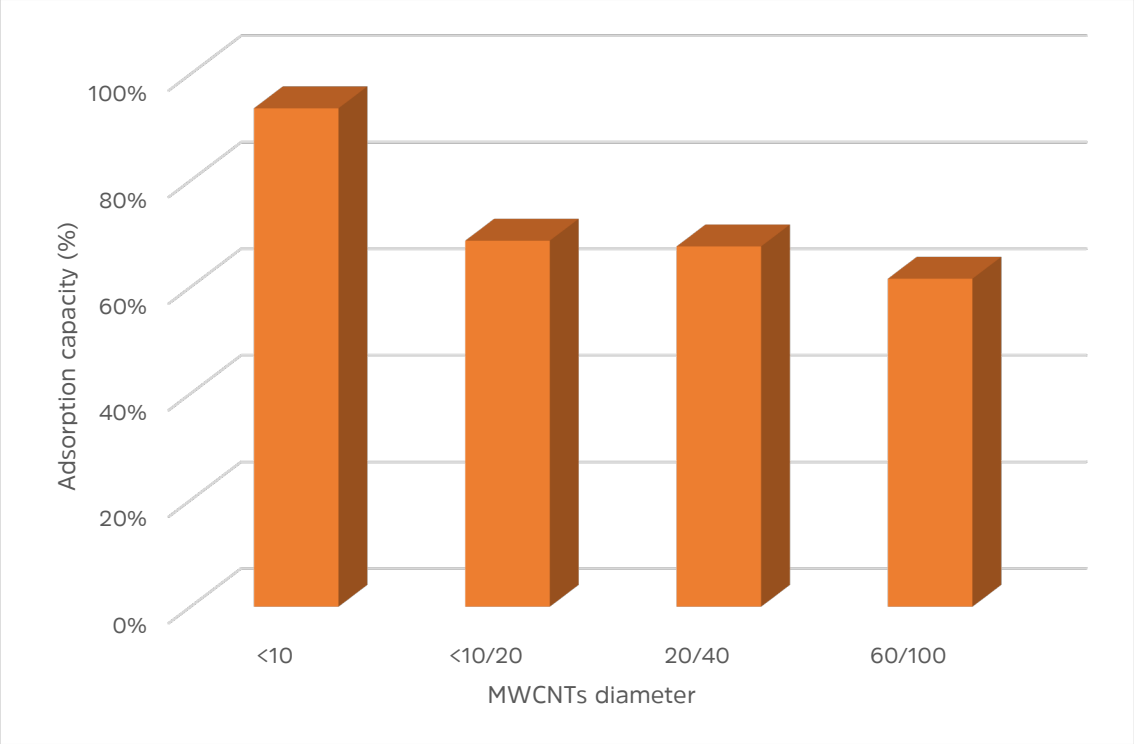

Figure 14 - Behavior of different diameter MWCNTs, promoting hydrophobic interactions for RNA extraction.

To further study the effect of MWCNTs diameter on the adsorption of more complex nucleic acid samples, the same conditions were used to promote hydrophobic interactions but using a mixture of RNA and DNA as sample. Adsorption results from the previous assay with only RNA, were also corroborated by the results obtained in the agarose gel electrophoresis, since smaller MWCNTs were able to capture more RNA from the complex sample. As shown in Figure 15, the supernatant represented in F3 from 60/100 MWCNTs presents a higher amount of nucleic acids that were not adsorbed than in F1, resulting from <10 MWCNTs. More importantly, this result also demonstrated that MWCNTs predominantly adsorbed RNA and only slightly interacted with DNA species, since comparing F1, F2, and F3, there is a greater difference in the level of RNA concentration that did not bind, but DNA species are equivalent in all samples. Actually, under these conditions, the selectivity that was achieved with <10 MWCNTs clearly suggests the potential of CNTs for the separation of different nucleic acids species. The adsorption occurs when the hydrophobic RNA bases interact with the sidewall of the MWCNT via π-stacking. Since DNA is double-stranded and has a tightly packed structure

with limited space availability of nitrogen bases, the interaction is not favored, resulting in preferential interaction of MWCNTs with RNA exposed bases.

It was clear at this point that MWCNTs <10 and experimental conditions that mainly promoted hydrophobic interactions were the ideal parameters to choose.

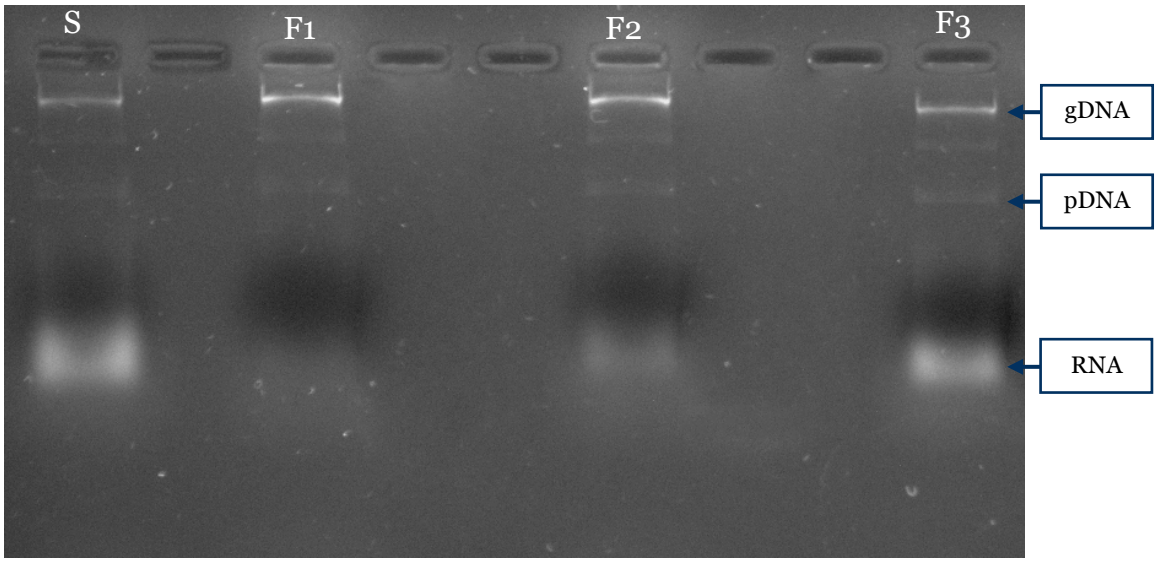

Figure 15 - Agarose gel electrophoresis of the supernatants recovered from MWCNTs adsorption assay, representing not bound species. S - Initial sample containing total nucleic acids (gDNA, pDNA and RNA); F1 – Supernatant recovered from <10 MWCNTs; F2- Supernatant recovered from 20/40 MWCNTs; F3- Supernatant recovered from 60/100 MWCNTs.

4.1.1. Effect of ionic strength on RNA adsorption

Since ionic strength is an important aspect for promoting hydrophobic interactions, it was increased the concentration of ammonium sulfate in equilibration/binding buffer to verify its effect on the adsorption of RNA onto MWCNTs. For that, 2.5 M $(NH_4)_2SO_4$ in 10 mM Tris-HCl pH 8 was used as equilibration/binding buffer for posterior comparison with the previously used binding buffer, 1.5 M $(NH_4)_2SO_4$ in 10 mM Tris-HCl pH 8. The results showed that this increase in the concentration of ammonium sulfate did not promote a significant increase in RNA binding (Figure 16), and therefore this option was discarded. Also, as described in 1998 by Lamers and co-workers, ammonium sulfate has a significant environmental impact since ammonium sulfate has a high eutrophication potential and is, therefore, difficult to dispose of. Thus, using the lower ammonium sulfate concentration was the best option either for the adsorption capacity and for the environmental perspective.

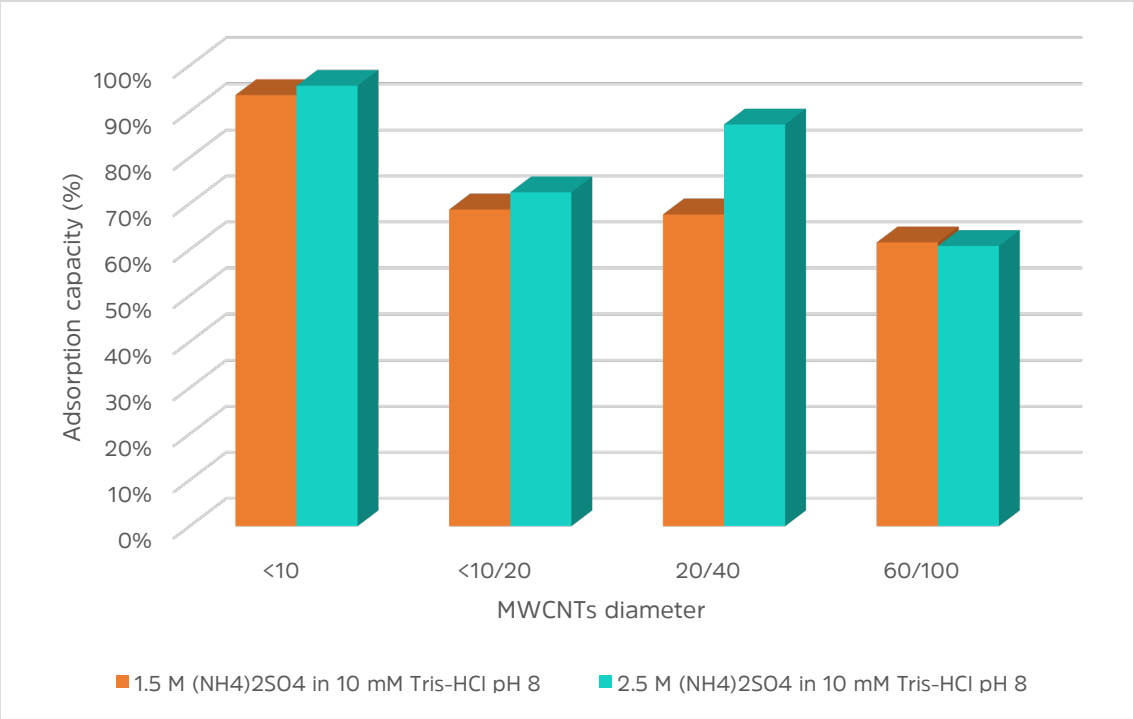

Figure 16 - RNA adsorption capacity for MWCNTs tested, at different ammonium sulfate concentration in equilibration/binding buffer. Two different buffers were used: 1.5 M $(NH_4)_2SO_4$ in 10 mM Tris-HCl pH 8 and 2.5 M $(NH_4)_2SO_4$ in 10 mM Tris-HCl pH 8.

4.1.2. Maximum RNA adsorption capacity

Since the adsorption sites of MWCNTs become saturated at a certain RNA level, this assay was performed to find the maximum quantity of RNA that <10 MWCNTs could capture. The experiment was carried out under the optimal adsorption conditions, previously achieved. The results presented in Figure 17 suggest that the highest adsorption capacity is approximately 175 mg RNA/g MWCNTs since when 200 µg of RNA were applied, a significant percentage of RNA was not adsorbed (Figure 17 C). Agarose gel electrophoresis also corroborates this result, as shown in Figure 18.

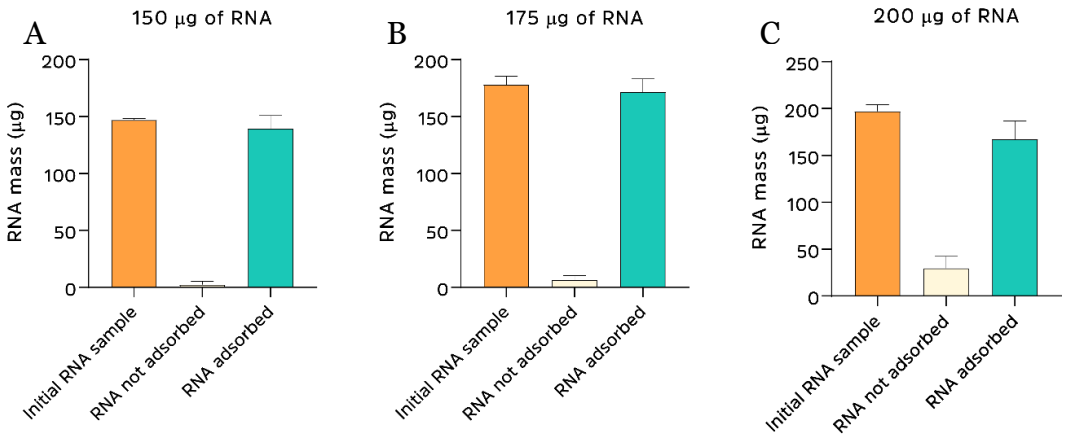

Figure 17 - Determination of maximum RNA adsorption capacity of <10 MWCNTs. A- Sample containing 150 µg of RNA; B- Sample containing 175 µg of RNA; C- Sample containing 200 µg of RNA. Values were calculated with the data obtained from three independent measurements (mean ± SD, n = 3).

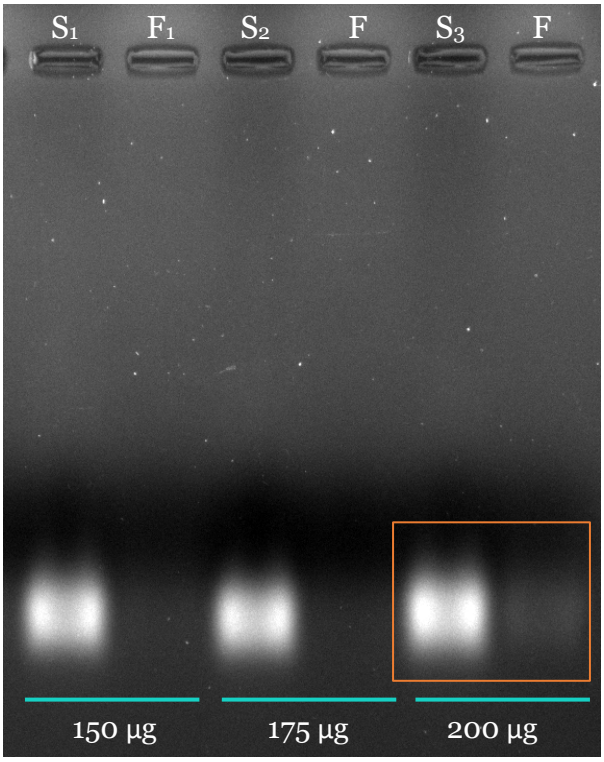

Figure 18 - Agarose gel electrophoresis representing adsorption of RNA onto <10 MWCNTs, for samples containing 150 µg, 175 µg, and 200 µg. S1-Initial RNA sample containing 150 µg; F1-Supernantant with non-adsorbed RNA; S2-Initial RNA sample containing 175 µg; F2- Supernatant with non-adsorbed RNA; S3-Initial RNA sample containing 200 µg; F3- Supernatant with non-adsorbed RNA.

A comparison of this capture approach, using as-grown <10 MWCNTs for RNA adsorption, with other reported methods was performed and is summarized in Table 6.

Table 6 - An overview of reported methods to isolate and extract nucleic acids.

Materials	Method	Extraction capacity (mg/g)	Molecule adsorbed	References
APBA attached-silica microspheres	UV-visible spectroscopy	60	RNA	[87]
Poly(HEMA-co-VPBA)	UV-visible spectroscopy	16	RNA	[88]
PEI-$FePO_4$	PCR	61.88	DNA	[89]
DES-mCS/MWCNTs	UV-visible spectroscopy	177.66	DNA	[60]
IL-Fe_3O_4	UV-visible spectroscopy	19.80	DNA	[90]
As-grown MWCNTs	UV-visible spectroscopy	175	RNA	This work

Analyzing the literature data, it is verified that there are already some methods to isolate and extract nucleic acids with different performances ranging from 16 mg/g to 177.66 mg/g. Although the diversity in performances, the extraction capacity does not differ depending on the molecule adsorbed, but on the strategy used, since for both RNA and DNA, there are systems with greater or lesser adsorption capacity. Indeed, MWCNTs with the conditions optimized in this work show comparable or better extraction than other published adsorbents.

4.2. Screening of conditions for the desorption/regeneration strategy

To further characterize the potential application of <10 MWCNTs, desorption experiments were carried out, as it was important to verify the possibility to recover the adsorbed biomolecules. Firstly, a mild desorption medium was tested to protect the structural integrity of RNA. For that, several buffers were evaluated. RNA with a concentration of 175 µg/mL was adsorbed onto <10 MWCNTs in 1.5 M $(NH_4)_2SO_4$ in 10 mM Tris-HCl pH 8.0, following the same protocol given previously. For the desorption experiments, Tris-HCl 10 mM at pH 8, Tween-20 at 0.5% and 1% (v/v), and sodium dodecyl sulfate (SDS) also at 0.5% and 1% (v/v), were evaluated. The results of RNA behavior regarding the desorption from MWCNTs were analyzed by absorbance measurement at 260 nm, and further calculation of desorption percentage.

The selection of the buffers for the desorption studies was based on the type of interactions established between RNA and the MWCNTs. As it was previously discussed,

the hydrophobic conditions were the main driving force for RNA adsorption, thus, the use of a decreasing ionic strength condition or the application of surfactants could be possible strategies for desorption. Surfactants, as amphiphilic molecules comprising both hydrophobic and hydrophilic moieties, could be able to compete with RNA by the MWCNTs surface. Moreover, these aqueous solutions avoid the use of organic solvents, thus making this method an eco-friendly one.

As represented in Figure 19, superior desorption was attained with surfactant solutions. Nonetheless, in none of the buffers used, the desorption was higher than 20%. This behavior can be explained on the basis of the strong interaction occurring, since the hydrophobic bases of RNA establish effective π-π interactions with π-cloud of MWCNTs surface; thus, promoting more effective retention in carbon nanotubes.

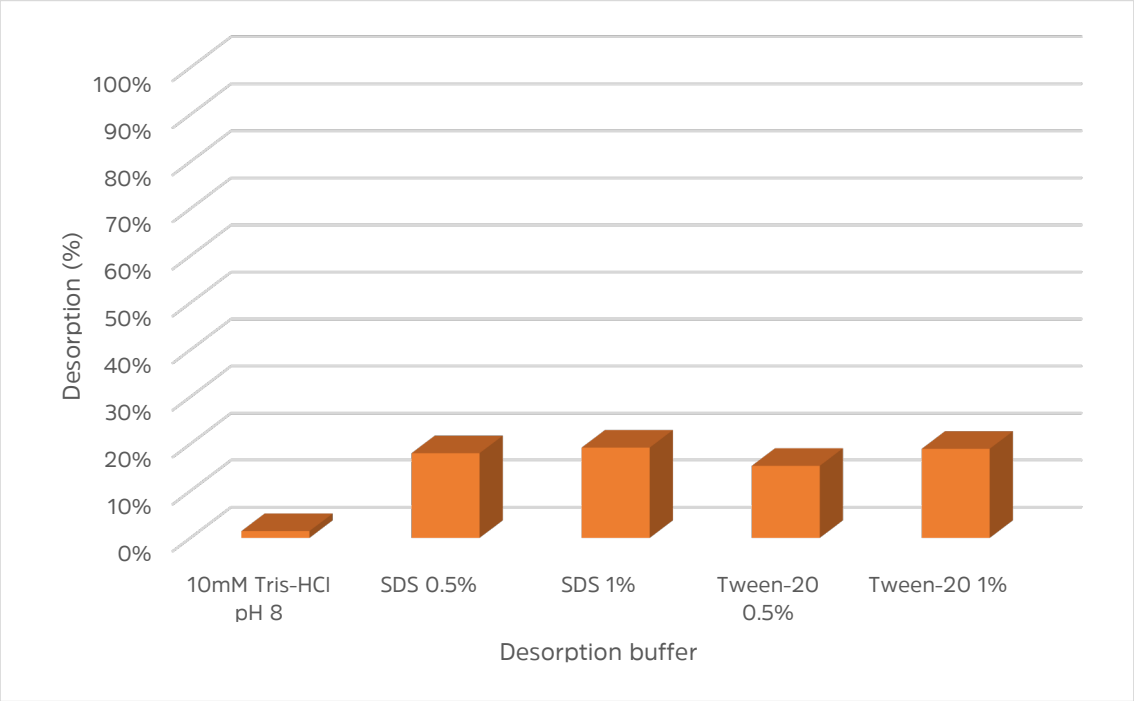

Figure 19 - RNA desorption with different buffers, namely, 10 mM Tris-HCl pH 8, SDS 0.5%, SDS 1%, Tween-20 0.5%, and Tween-20 1%.

Other strategies were also evaluated, namely by testing the inclusion of a washing step with deionized water, represented in Figure 20, or the use of sonication, represented in Figure 21. For the first experiment, all sizes of MWCNTs were tested. After applying 10 mM Tris-HCl at pH 8, 1 mL of deionized water was added to MWCNTs and left for 20 minutes in agitation. For the sonication assay, the <10 MWCNTs were tested, being

subjected to different sonication times (5 min, 10 min, and 20 min). The results presented show that neither the washing step nor the sonication step were efficient on the RNA removal from MWCNTs, being even less effective than surfactants. Moreover, with the sonication strategy, it was verified some destabilization or degradation of MWCNTs, difficulting separation between solid-phase and supernatant. Rossel and the research team, in 2013, discovered that sonication treatment could substantially change the sp2 structure of CNTs by introducing defect sites at their sidewalls, and consequently, changing their aspect ratio [91]. In 2018, Arrigo and co-workers described that the reduction of length of CNTs strongly influences the nanocomposite rheological behavior, which progressively alters from solid-like to liquid-like as the CNT sonication time increases [92]. This clearly evidenced that it was not an effective method for the recovery of nucleic acids adsorbed onto MWCNTs.

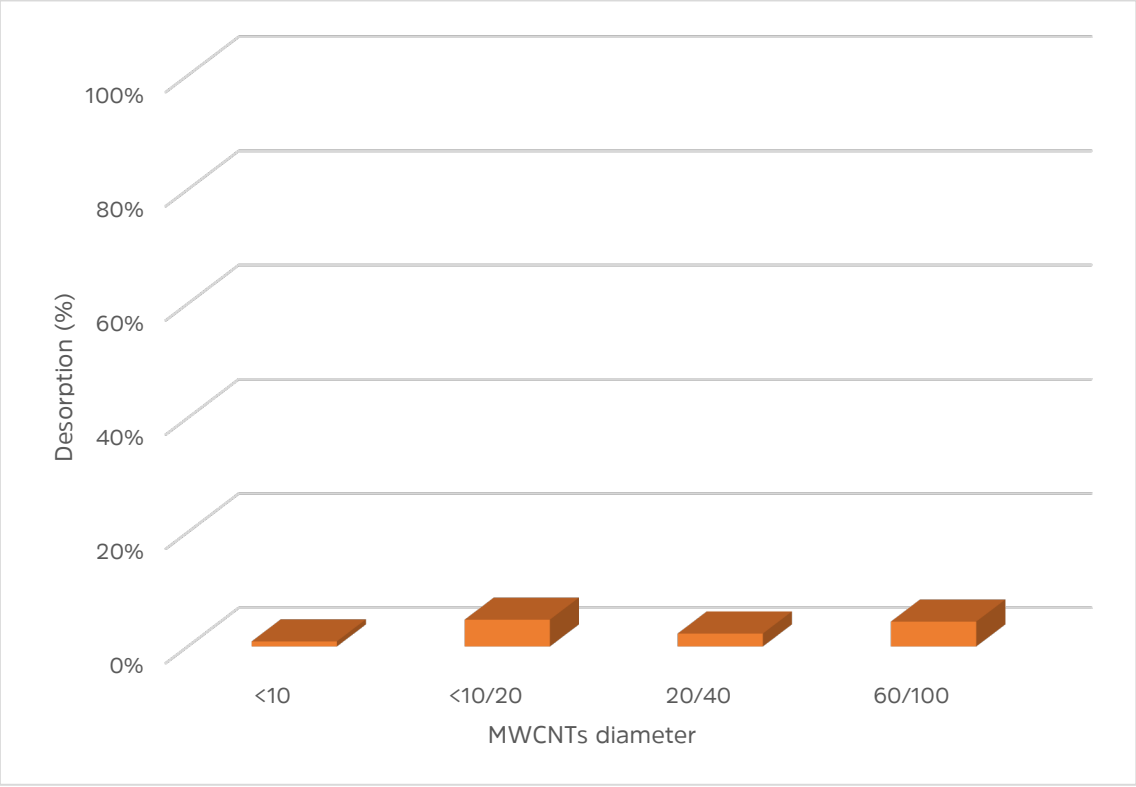

Figure 20 - RNA desorption from MWCNTs with different diameters, when applying 10 mM Tris-HCl pH 8 with an additional washing step with deionized water.

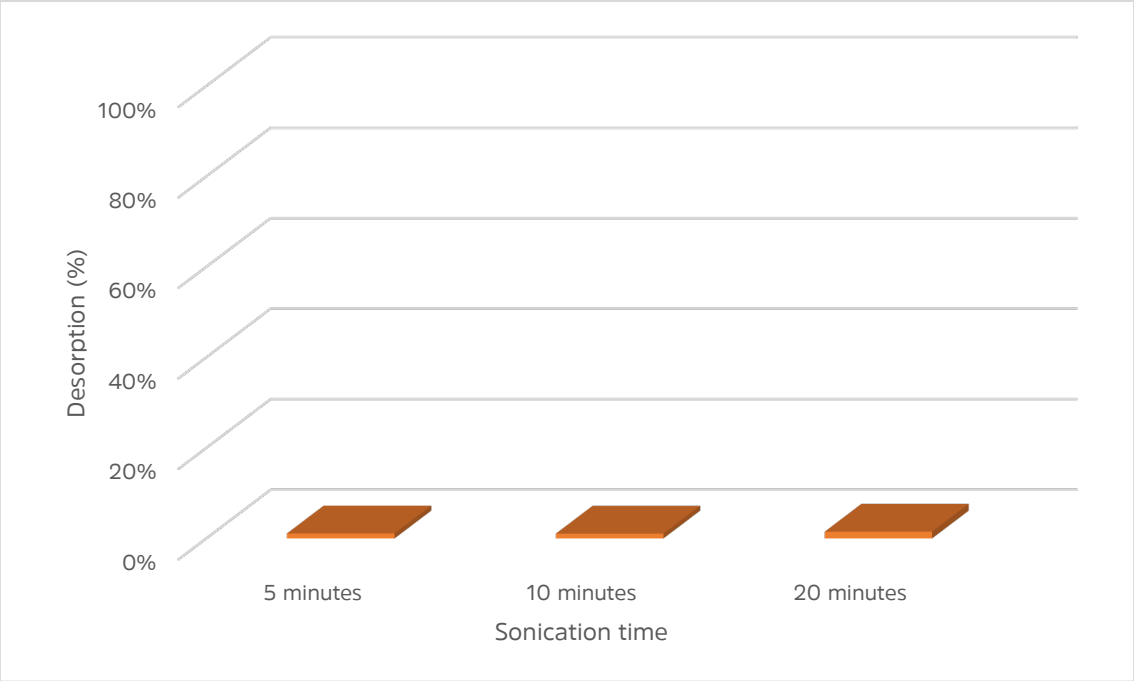

Figure 21 - RNA desorption when applying 10 mM Tris-HCl pH 8 with an additional sonication step for 5, 10, and 20 minutes.

At this point, it was clear that a soft strategy was not enough to successfully desorb RNA from MWCNTs, and the use of more effective but harsh conditions would imply the loss of RNA stability. So, the focus of the work shifted from trying to capture RNA for further use, to try to clarify pDNA, removing contaminants from a complex sample, including RNA, as it was already known that ability of CNTs. Thus, more harsh strategies to regenerate MWCNTs were evaluated, expecting to achieve a suitable strategy to recycle CNTs. Here, the degradation of RNA was not a concern since the aim was to regenerate the nanotubes to enable more uses, making this method more cost-effective.

Firstly, 1 M NaOH was evaluated for one-step regeneration, as this is a commonly established strategy for regeneration and sanitization of materials ([93]), but a two-step strategy was then applied, since the results of one-step regeneration were not favorable. The previously tested surfactants were used for the first regeneration step of this approach since they were the most promising buffers for desorption. After centrifugation and removal of the first buffer, 1 mL of 1 M NaOH was applied to MWCNTs and homogenized for 20 minutes. After centrifugation and removal, the absorbance of the aqueous phase was measured. The results in Figure 22 indicate a significant removal of bound material from MWCNTs surface with this two-step regeneration strategy for all surfactant buffers, all reaching near 100 % of desorption. Afterwards, a new adsorption experiment was performed, with the regenerated MWCNTs to verify if adsorption

occurred (after regeneration) and validate the regeneration protocol. The results in Figure 23 demonstrate that adsorption of RNA after regeneration of MWCNTs is maintained and the adsorption capacity is not significantly compromised, mainly when using Tween-20 0.5% + 1 M NaOH as desorption strategy, as the second experiment revealed an adsorption capacity of around 90%.

In general, Tween-20 0.5% with 1 M NaOH seemed to be the most promising regeneration strategy and was used for the subsequent assays.

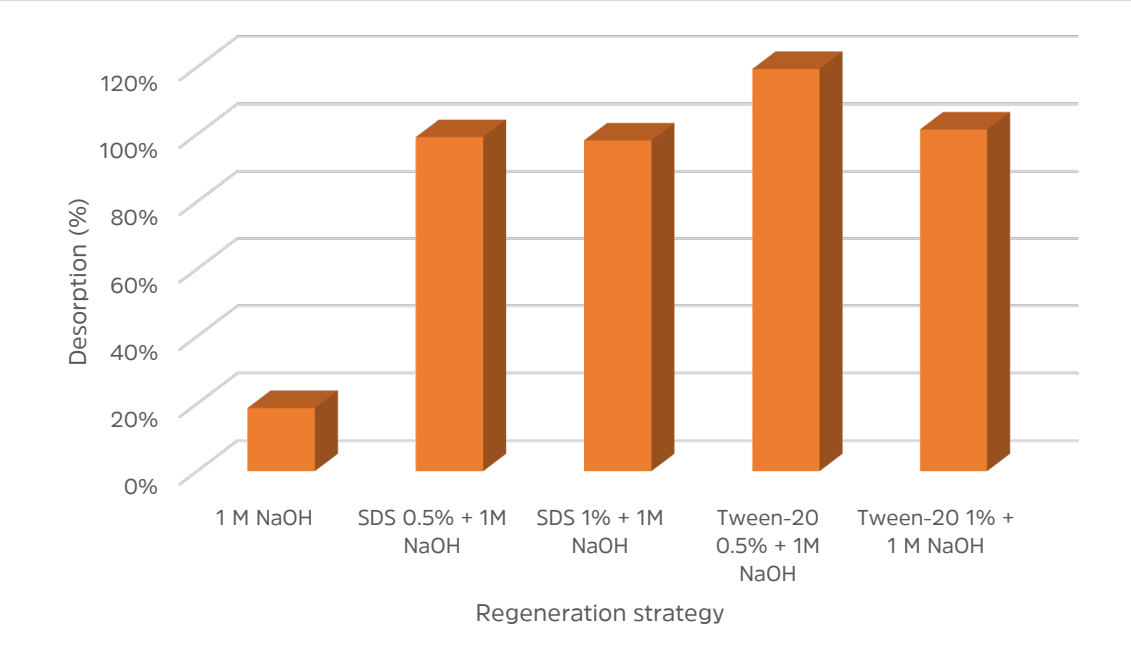

Figure 22 - RNA desorption when applying 1 M NaOH as a single regeneration step or combining this step with a second condition comprising the use of surfactants.

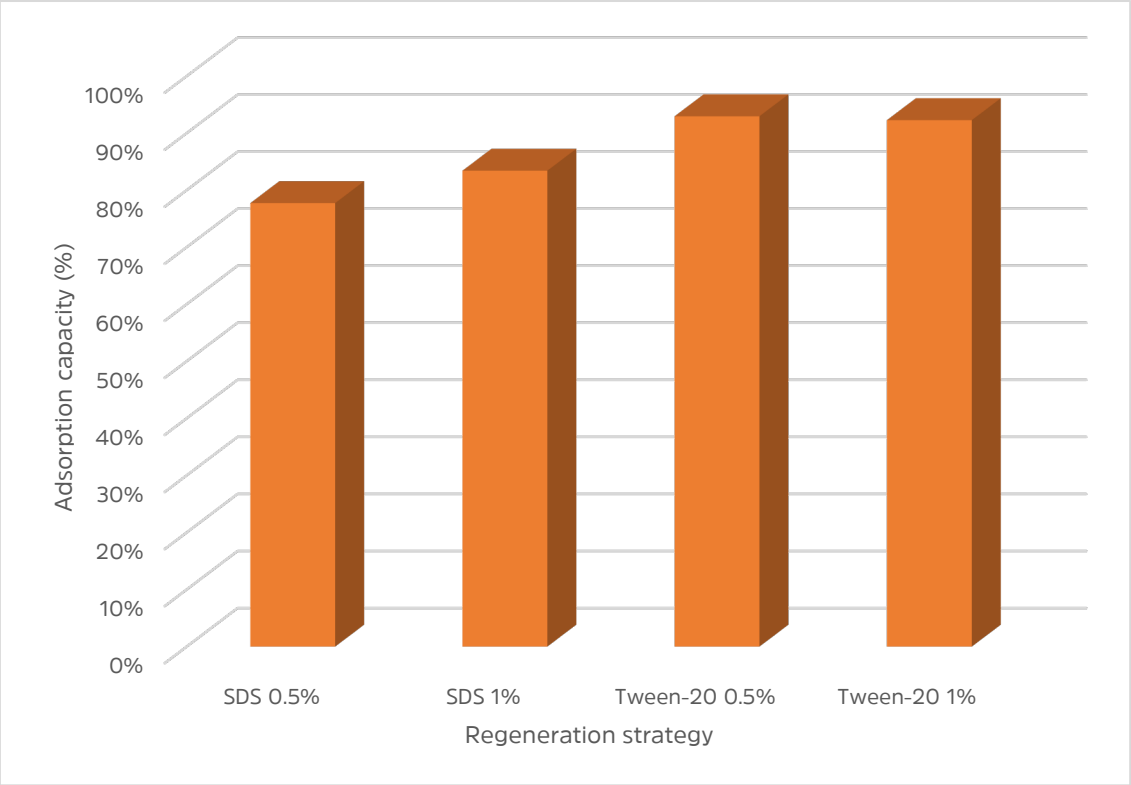

Figure 23 - RNA adsorption capacity after MWCNTs regeneration through different strategies.

4.3. Reuse of MWCNTs

For potential applications, the reuse of an adsorbent is an essential factor to be reported. Once completed the adsorption/ desorption strategy screening, it was time to improve this technology and further reduce its environmental impact and reduce costs. Thus, the possibility of recycle and reuse MWCNTs was assessed. After regeneration, MWCNTs were recovered and used to capture RNA again. For this, the same strategy as the previous assay was used, and a 1 mL RNA sample, with a concentration of 175 µg/mL was applied to MWCNTs. Figure 24 shows that the capture capacity is maintained with a slight decrease after the second cycle and a higher loss after three cycles, where the adsorption did not surpass the 50%. This loss of adsorption capacity can be related to some loss of sorbent material resulting from all centrifugations and pipetting required. Also, progressive oxidation of MWCNTs by 1 M NaOH could decrease RNA adsorption capacity [94]. The oxidation phenomenon can lead to a rise of MWCNT hydrophilicity, and consequently, a loss in RNA adsorption ability. In 2012, Doepke and collaborators described the possibility of as-grown MWCNTs suffer oxidation in a 1 M sodium hydroxide solution. They also reported that the addition of polar groups during oxidation

led to a significant change in MWCNTs surface chemistry, and consequently, MWCNTs shifted from hydrophobic to a hydrophilic surface [94].

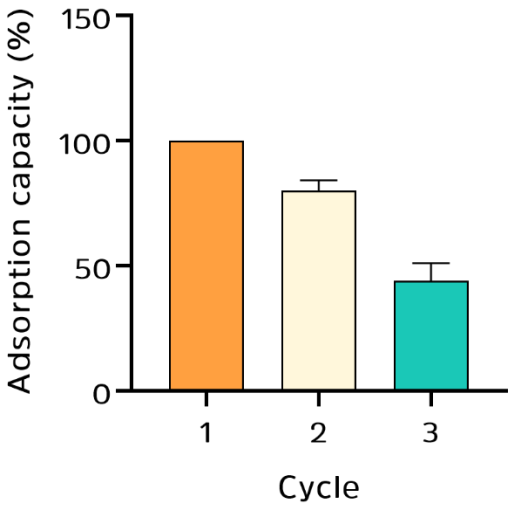

Figure 24 - RNA adsorption capacity when employing 1 mg of <10 MWCNTs for three consecutive assays. Values were calculated with the data obtained from two independent measurements (mean ± SD, n = 2).

To evaluate the behavior of MWCNTs in a complex sample, experiments with an *E. coli* lysate sample comprising a concentration of around 2800 μg/mL were performed. In this case, the same MWCNTs were used for three consecutive cycles with the application of a new sample at the start of each run, and the results were analyzed by absorbance measurement and agarose gel electrophoresis. This assay allowed the investigation of MWCNTs adsorption performance through different runs and the study of selectivity between RNA and pDNA in a complex matrix.

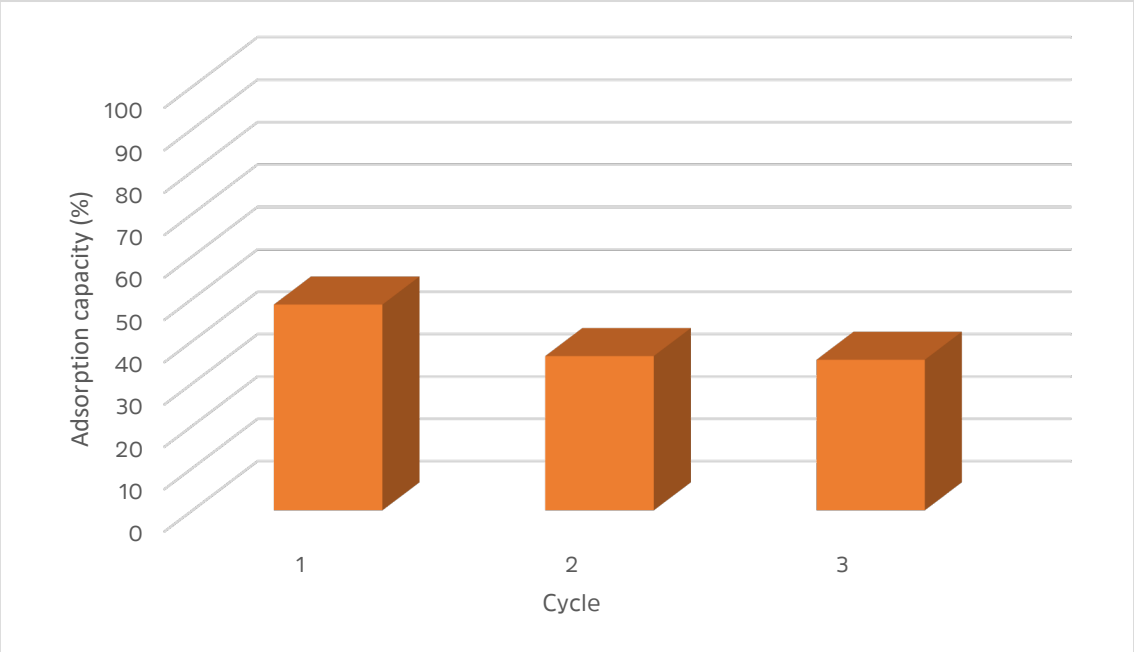

Figure 25 - MWCNTs adsorption capacity when a complex E. coli lysate sample is applied for three consecutive cycles.

As represented in Figure 25, MWCNTs have the capacity of removing approximately half of all lysate material in the first cycle, with a slight decrease in the second cycle, maintaining almost the same capacity of adsorption through all three runs, thus confirming a good stability of MWCNTs after regeneration, proving the effectiveness of the strategy. With agarose gel electrophoreses (Figure 26), it was possible to see that even in a complex matrix, MWCNTs have an apparent selectivity between RNA and pDNA, since, in all three cycles, there is a significant difference between the initial sample (Figure 26 S1, S2, and S3) and the final clarified sample (Figure 26 F1, F2, and F3), where a significant amount of RNA was adsorbed, leaving pDNA in the aqueous-phase. This is visible by comparing the band intensity, being verified that the pDNA bands are similar between the initial samples and samples resulting from adsorption experiments, while the RNA bands are significantly fainter after MWCNTs adsorption.

Then, a different experiment was performed, using the same MWCNTs along the three cycles, but regarding the sample it was first used the complex lysate and then the supernatant resulting from the first cycle was applied in a second cycle, and the sample resulting from the second cycle was applied in a third run. With this experiment, it was possible to test the potential of a single batch of MWCNTs to thoroughly remove RNA from a complex sample. By agarose gel electrophoresis (Figure 27), it is possible to see that the procedure optimized in this work can be useful to substantially improve the purity of the pDNA sample. Comparing with the initial sample (Figure 27 S1), it is clear

the decrease on the intensity of the RNA band after each cycle. Thus, with only three cycles, 1 mg of MWCNTs, were able to capture all RNA present in *E. coli* lysate sample, improving the pDNA purity.

The extraction of pDNA from *E. coli* cell lysate is already described in the literature. For instance, in 2004, Kepka and co-workers developed an ATPS system [(50% ethylene oxide–50% propylene oxide)–Dextran T 500] for the partitioning of the different nucleic acids from *E. coli* lysate. This method enabled the recovery of the pDNA and a 54% removal of total RNA from the sample. Then, an optimization was performed to reduce the top-phase volume and the RNA removal efficiency was improved to 80% [95].

In comparison, and using our method based on MWCNTs, it was possible to completely remove RNA from *E. coli* lysate sample without diluting pDNA and without using large amounts of toxic solvents. Furthermore, depending on the intended application, the strategy allows to include additional cycles, enabling to increase the final purity of the pDNA. Nevertheless, further investigation is required to improve performance after recycling and extend the lifetime of MWCNTs to more runs.

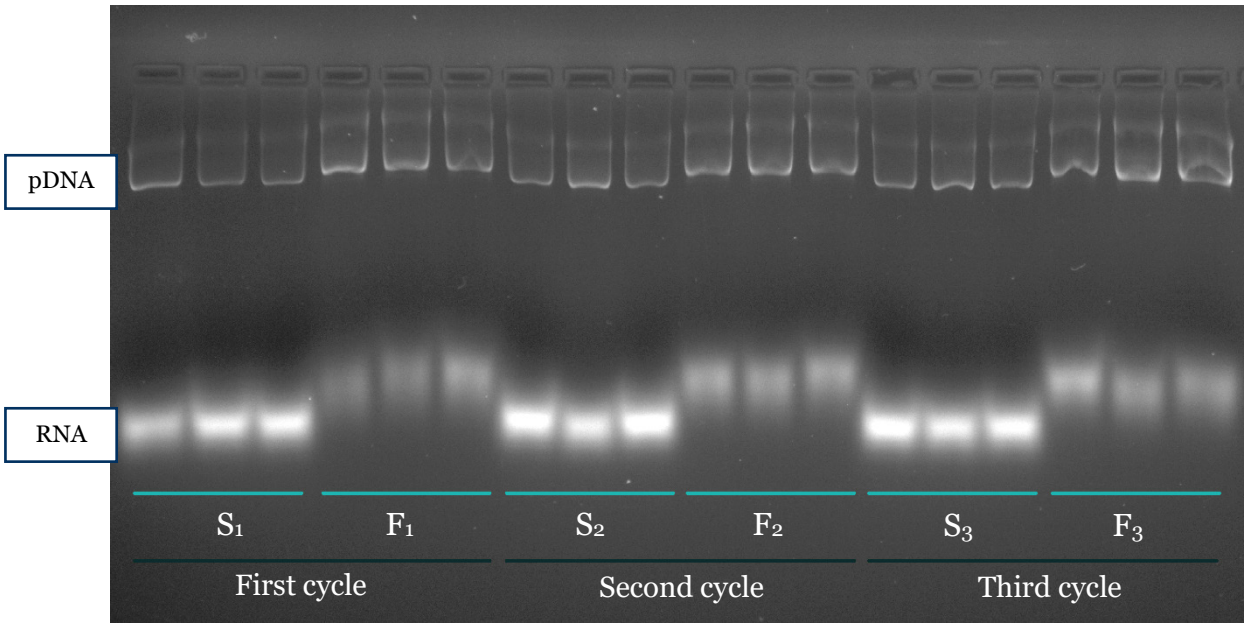

Figure 26 - Agarose gel electrophoresis of *E. coli* lysate before and after <10 MWCNTs adsorption procedure for three independent cycles. Three independent assays were performed (n=3). S1-Initial *E. coli lysate* sample for the first cycle with <10 MWCNTs; F1-Sample containing non-adsorbed species after first cycle on MWCNTs; S2-Initial *E. coli lysate* sample for the second cycle with <10 MWCNTs; F2-Sample containing non-adsorbed species after second cycle on MWCNTs; S3-Initial *E. coli lysate* sample for the third cycle with <10 MWCNTs; F3-Sample containing non-adsorbed species after third cycle assay on MWCNTs.

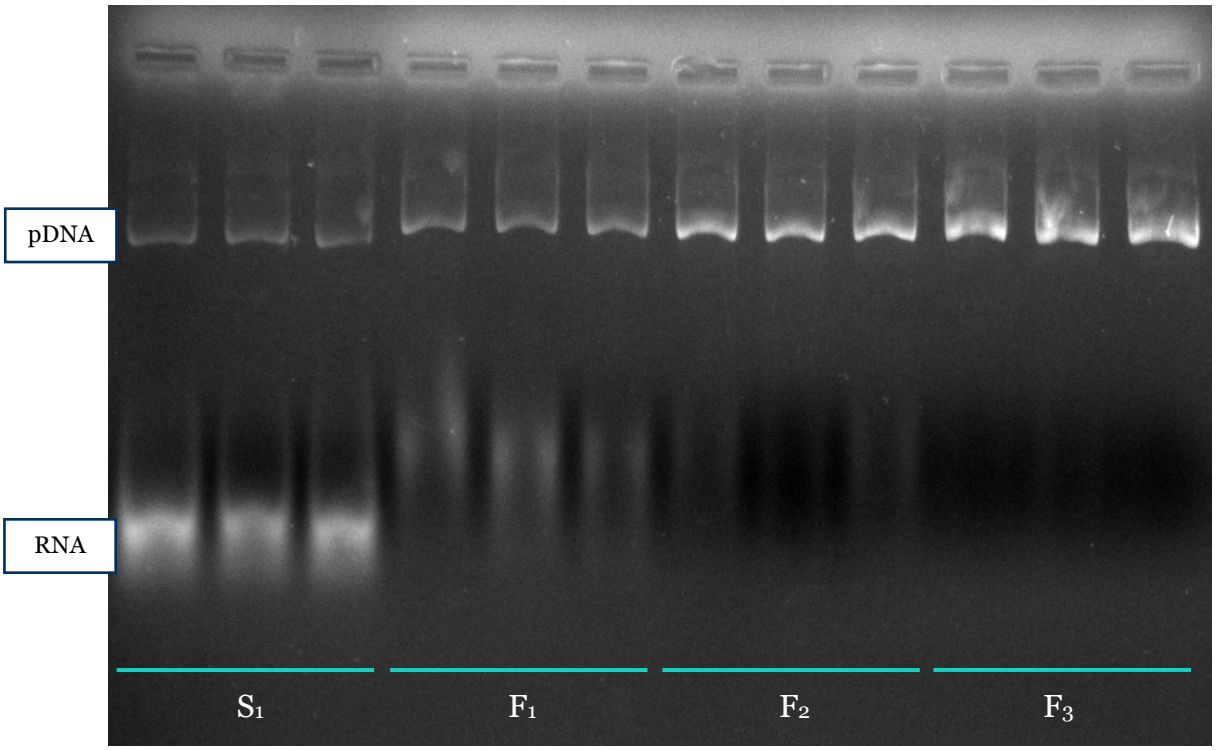

Figure 27 - Agarose gel electrophoresis of *E. coli* lysate before and after <10 MWCNTs adsorption procedure for three consecutive cycles. Three independent assays were performed (n=3). S1-Initial *E. coli* lysate sample for the first adsorption cycle with <10 MWCNTs; F1-Sample after first cycle assay, comprising all solutes not adsorbed onto MWCNTs; F2-Sample after second consecutive cycle assay comprising all solutes not adsorbed onto MWCNTs; F3-Sample after third consecutive cycle assay comprising all solutes not adsorbed onto MWCNTs.

4.4. Cytotoxic of MWCNTs

Since in this work, the primary goal is to isolate pDNA for use as a biopharmaceutical product, it is essential to test any cytotoxic effect that MWCNTs might present since, although not expected, some adsorbent material can remain in the sample. In this sense, the colorimetric assay MTT was used to assess human fibroblasts (hFIB) viability in the presence of MWCNTs in three different quantities, 25, 50, and 100 µg. By analyzing Figure 28, it is confirmed that hFIB were maintained in culture in contact with MWCNTs for 24h and 48h in which it was possible to verify that they did not induce any cytotoxic effect on these cells. It is important to note that at 48h, for 100 µg of MWCNTs it is possible to observe that cell viability was below the negative control, but since viability was still above 80% it does not represent cytotoxicity. However, even if some residual amount of CNTs remain in the pDNA sample, it would not be at a concentration this high, which further confirms the safety of the material for this clarification/pre-purification application.

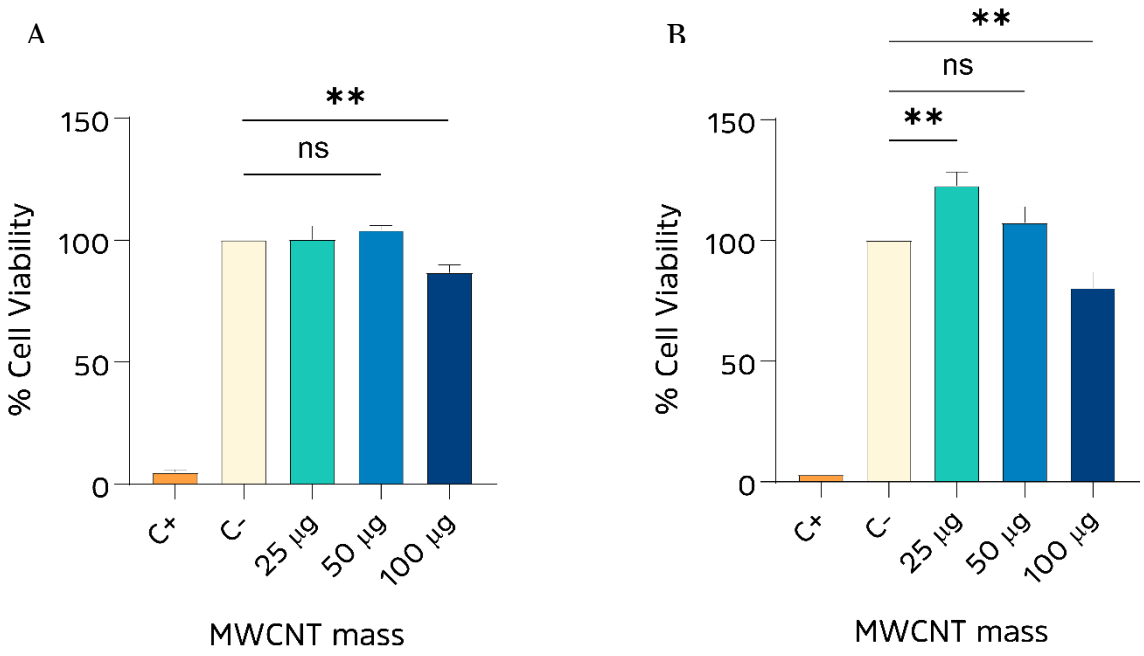

Figure 28 - Cellular viability by MTT assay of human fibroblasts after 24 (A) and 48 hours (B) incubation with 25, 50, and 100 µg of as-grown <10 MWCNTs. The negative control (C-) comprised untreated cells and positive control (C+) were treated with ethanol 70%. Viability percentage is expressed relatively to the control cells. Values were calculated with the data obtained from three independent measurements (mean ± SD, n = 3). Statistical analysis was performed using "One-way ANOVA". Significant differences are indicated as: (ns = $p > 0.05$; **** $p \leq 0.0001$; *** $p \leq 0.001$; ** $p \leq 0.01$; * $p \leq 0.05$); and determined with Tukey's multiple comparisons.

4.5. Selectivity between RNA and pDNA

To further evaluate the separation between RNA and pDNA additional experiments were performed, also intending to analyze the influence that both RNA and pDNA have in RNA capture by the MWCNTs. For these experiments, RNA and pDNA mixtures were prepared with final concentrations of 175 µg/mL (Figure 29 A), 350 µg/mL (Figure 29 B), and 500 µg/mL (Figure 29 C), but combined in three different ratios: 25% RNA/75% pDNA; 50% RNA/50% pDNA; 75% RNA/25% pDNA. Through the analysis of agarose gel electrophoresis, it was possible to observe that the concentration of both DNA and RNA does not influence RNA capture, and even when a small concentration of RNA is present in the sample, apparently pDNA does not adsorb onto MWCNTs, considering the conditions in study. When using a mixed sample with a final concentration of 500 µg/mL (Figure 29 C), it was tested the addition of a second cycle, since not all RNA was captured in the first cycle due to its higher concentration. This second cycle proved to be effective in removing additional RNA, contributing to greater clarification of the pDNA, without compromising selectivity.

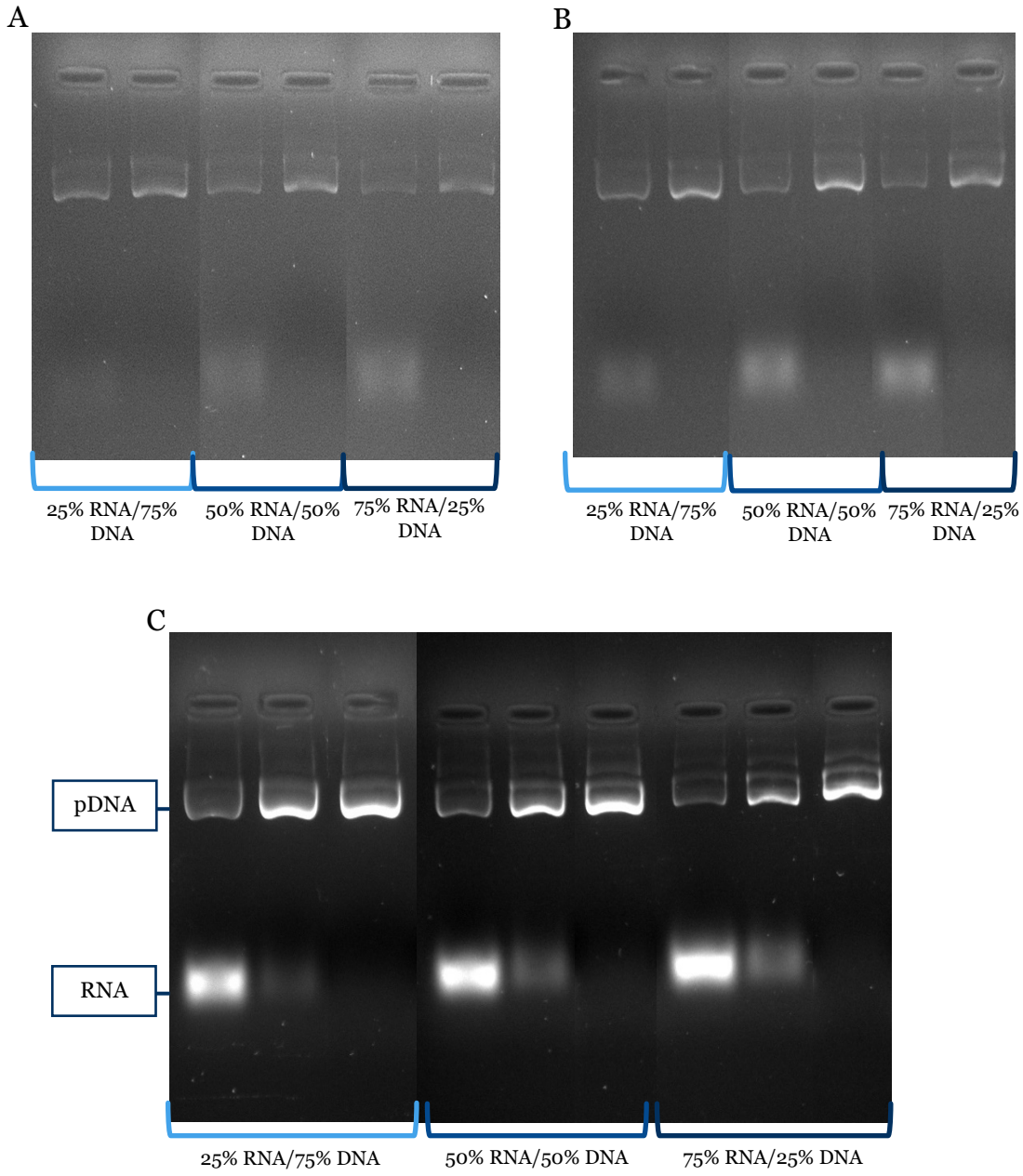

Figure 29 - Agarose gel electrophoresis of RNA and DNA mixtures before and after <10 MWCNTs extraction procedure with three different ratios. A: 175 µg/mL; B: 350 µg/mL; C: 500 µg/mL. S1-Initial sample; F1-Sample after first adsorption cycle, comprising all solutes not adsorbed to MWCNTs; F2-Sample after second adsorption cycle comprising all lysate solutes not adsorbed to MWCNTs.

The robustness and potential of MWCNTs adsorption capacity were demonstrated through this experiment, since it was showed the possibility of being applied even to more concentrated samples, as demonstrated with 75% RNA/25% pDNA ratio, without losing selectivity.

4.6. Quantification of pDNA

Another crucial aspect for the validation of this pDNA clarification procedure is to understand if some pDNA unspecifically adsorbs onto the carbon nanotubes, as this could represent the loss of pDNA and a decrease in its recovery yield. Although selectivity has already been verified and analyzed by qualitative methods, it was essential to quantify the fraction of pDNA that could be lost. Therefore, an assay was performed, with the same conditions optimized before, but with a pDNA sample (Figure 30). For a more accurate analysis and quantification of pDNA, an analytical chromatographic assay was carried out, using the CIMac monolithic column. For this, a pDNA control sample with 175 μg/mL of concentration was injected onto the column, and the same sample was subjected to the established adsorption protocol with MWCNTs, to further quantify the pDNA that remains in the supernatant (not adsorbed pDNA). Through the analysis of the peaks, it could be seen that there was a slight reduction in the peak size corresponding to the pDNA after the clarification process. By integrating the peaks, it was possible to obtain their areas and determine the quantity of pDNA lost. Table 7 shows the peak area data, as well as the corresponding concentration. It is possible to verify that using MWCNTs to clarify the pDNA sample, 86% of pDNA remains in the supernatant, while 13.9% of pDNA is adsorbed onto MWCNTs, representing some loss of pDNA. Compared with other reported methods for isolation of pDNA, this approach shows similar or better results when analyzing the percentage of pDNA recovered. Liu (2012) used gold nanoparticles and graphene oxide for DNA isolation and reported a recovery of approximately 80% of DNA during the procedure [96]. In a similar work, Chen and co-workers reported a 31% of pDNA recovered when using hemoglobin modified magnetic nanocomposites as a solid-phase adsorbent for isolation of pDNA [97]. Thus, considering the efficiency in pDNA clarification, as-grown MWCNTs and the method here described can be effectively used.

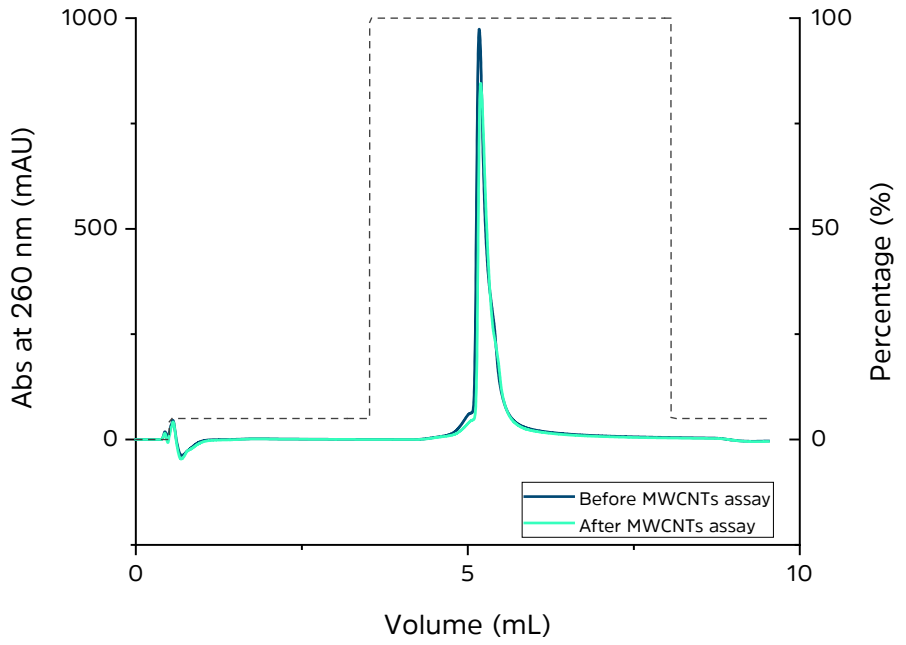

Figure 30 - Representative chromatogram of pDNA after MWCNTs clarification procedure. The peak with dark blue represents pDNA before clarification procedure and the peak with light green line represents pDNA after clarification procedure.

Table 7 - Assessment of peak area and corresponding pDNA concentration.

	Peak area	[pDNA] (µg/mL)
Control pDNA	225.8	206
pDNA after clarification by MWCNTs	195.8	178

4.7. The integrity of pDNA after the clarification procedure

To assess the integrity and stability of plasmid DNA recovered from the MWCNTs extraction procedure, a circular dichroism (CD) analysis was performed. For comparison purposes, it was analyzed a pDNA control sample (purified by a commercial kit), and the pDNA that was recovered from the supernatant (not bound species) of the adsorption experiment done with MWCNTs. Figure 31 shows that both curves have similar shapes with a negative band near 245 nm and two positive bands at 220 and 275 nm, which are

the characteristics bands of DNA, corresponding to π- π base stacking and DNA helicity. The results indicate that no significant alterations in the secondary structure of pDNA occur, during the clarification process with CNTs. Hence, the extraction procedure does not compromise pDNA integrity, allowing to maintain its native conformation.

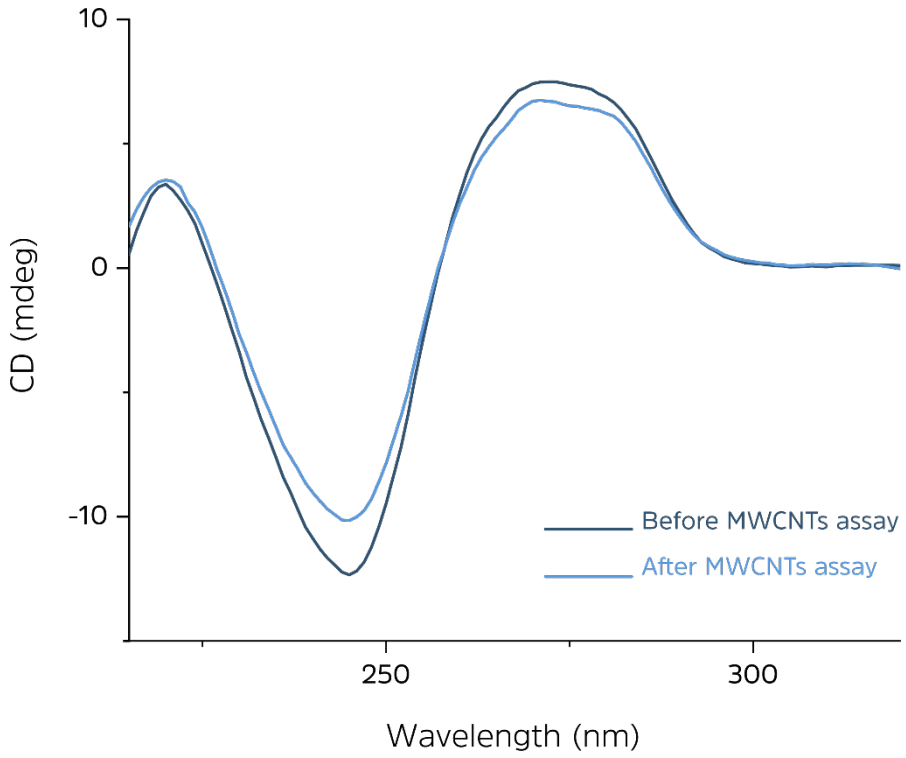

Figure 31 - CD spectra from 210 to 320 nm, of pDNA before and after MWCNTs extraction assay. Dark blue line represents control pDNA before the extraction procedure and light blue line represents pDNA after extraction procedure.

4.8. Clarified pDNA quality control

The *E. coli* lysate sample used in assays was not clarified, presenting a great diversity of biomolecules, like RNA, gDNA, proteins, endotoxins, and other impurities. These impurities represent more than 90% of the total mass of solutes and should be substantially cleared from the sample, in order to recover pure pDNA. Hence, several assays were performed to assess the capability of MWCNTs to remove impurities and clear up the pDNA sample.

4.8.1. Total protein quantification

It is reported that *E. coli*, the primary host for pDNA production, comprises around 4300 protein-coding genes [98]. Given this diversity, the removal of these biomolecules must be considered since they pose some risks and can induce immunogenic responses, upon administration of biopharmaceuticals. In 2003, Wang's research group demonstrated that several peptides presented affinity and could bind non-covalently through hydrophobic interactions to carbon nanotubes [99]. Since then, many studies have shown the capability of CNTs to adsorb proteins. In this regard, quantification of protein was performed through the Bradford protein assay on the clarified *E. coli* lysate after the clarification procedure with MWCNTs. The results suggested that a significant protein capture is also obtained with as-grown MWCNTs reducing by almost half the quantity of proteins initially present in the lysate sample (Table 8). It was also tested the performance of the same batch of MWCNTs for protein removal for three consecutive assays, applying a new *E. coli* lysate sample at the start of each cycle, as it is represented in Figure 32. The results are auspicious since MWCNTs showed to maintain their performance on reducing protein levels throughout all assays.

Table 8 - Total protein amount of the crude *E. coli* lysate and the clarified lysate after MWCNTs capture procedure. Values were calculated with the data obtained from three independent measurements (mean ± SD, n = 3).

Samples	[Protein] (μg/mL)
Crude *E. coli* lysate	300
Clarified lysate after extraction	178

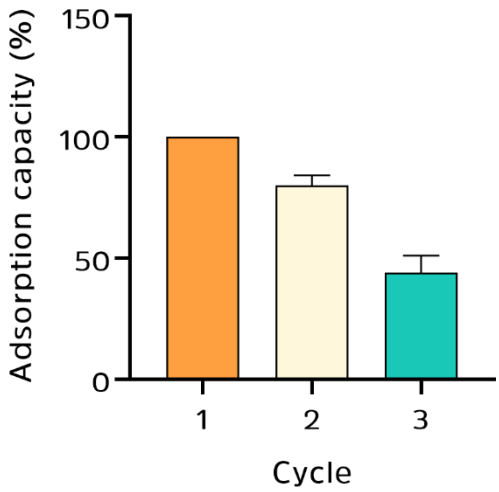

Figure 32 - Protein adsorption capacity by <10 MWCNTs through three consecutive cycles. Values were calculated with the data obtained from three independent measurements (mean ± SD, n = 3).

4.8.2. Genomic DNA quantification

Genomic DNA in biopharmaceutical products always presented a concern for regulatory agencies and the biopharmaceutical industry. The main apprehension here is that residual fragments of foreign gDNA can be inserted into the genome of the patient [47]. In this regard, it is of the utmost importance to remove residual levels of this molecule from the pDNA biopharmaceutical sample. If this reduction could be achieved since the first clarification steps, would be of great advantage, as it would simplify the downstream processing for further purification of pDNA. Quantification of gDNA present in the clarified lysate and in the pDNA sample recovered from the clarification step with MWCNTs was performed by qPCR. The results presented in Table 9 show that the clarification procedure reduces approximately 6 times the gDNA concentration present in *E. coli* lysate, going from 160 µg/mL in the initial lysate sample to 26 µg/mL after the clarification procedure. Witek and research team (2006) reported a purification and preconcentration of gDNA from *E. coli* cell lysate using photoactivated polycarbonate microfluidic chips. After the recovery process capture efficiency of gDNA was estimated to be 39% for 0.05 mg/ml *E. coli* cell suspension, and 85% when the cell suspension concentration was set below 0.02 mg/ml [100]. In this work, through MWCNTs it was obtained a gDNA reduction of approximately 84%. Despite being a clarification step, a significant reduction of gDNA is achieved, what can greatly simplify the subsequent purification stage.

Table 9 - Quantity of genomic DNA on the crude *E. coli* lysate and in the clarified lysate after MWCNTs procedure. Values were calculated with the data obtained from three independent measurements (mean ± SD, n = 3).

Samples	[gDNA] (µg/mL)
Crude *E. coli* lysate	160
Clarified lysate after MWCNTs	26

4.8.3. Overall analysis of contaminants

Once completed the quantification and assessment of the major contaminants present in the sample, a more global analysis was made. Through the AKTA Pure equipment, it was performed several sample injections onto CIMac analytical column. For this assay, it was again used the *E. coli* lysate as a sample, and three consecutive clarification cycles were performed, with the same sample, to see the differences in chromatographic profile between the initial sample and subsequential runs. Represented in Figure 33 are the chromatographic profiles of the initial sample and three consecutive cycle samples. The first peak comprises all contaminants present in the sample that do not interact with the column. On the other hand, the second peak appears after applying the elution buffer and includes some contaminants and pDNA. From the analyses of the chromatographic profile, it is possible to verify that this extraction procedure has the potential to remove a significant amount of impurities, not significantly altering the pDNA corresponding peak throughout the three cycles.

After all quantification analyses, an estimate was made of the percentage of each studied constituent of the lysate sample to help visualize the impact of this technology on reducing contaminants. This representation is presented in Figure 34. After the clarification procedure, all impurities are substantially cleared out, and a pDNA-enriched sample is obtained. As Prazeres (2011) referred in his work, the intermediate recovery step has the main objective of clarifying impurities to end up with a solution where pDNA accounts for approximately 50% of all solutes, reducing the burden imposed on the high-performance/high-cost unit operations [47]. Overall, this process presents good efficacy since the percentage of pDNA in the clarified sample is around 50%.

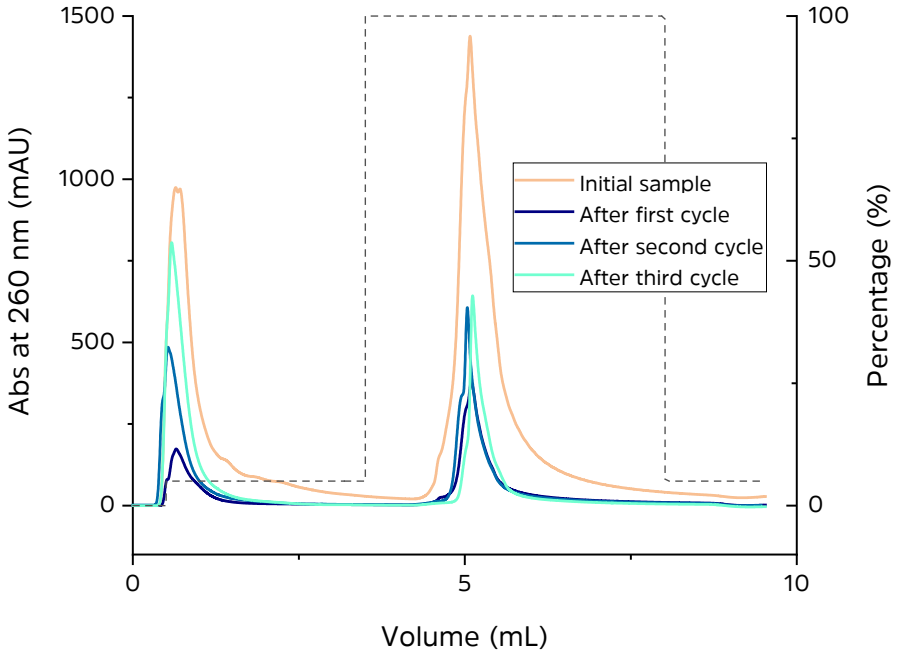

Figure 33 - Representative chromatogram of *E. coli* lysate before and after <10 MWCNTs clarification procedure thorough three consecutive cycles.

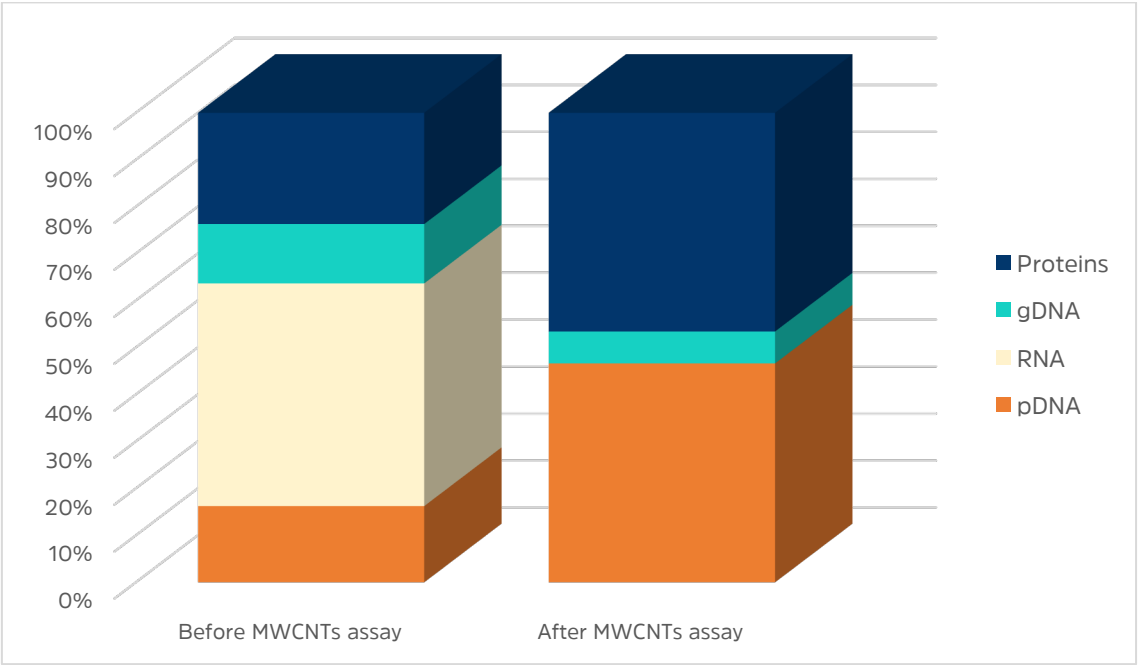

Figure 34 - Graphical representation of the estimated percentage of studied constituents present in *E. coli* sample, before and after MWCNTs clarification procedure.

CHAPTER 5

5. Conclusions and Future Perspectives

The demand for plasmid DNA for both gene therapy and vaccine development has been immense. This exponential interest led to the necessity to develop efficient purification strategies of these biomolecules to obtain them with total integrity, highly pure, and biologically active. To respond to this challenge, carbon nanotubes were explored as a new promising tool for clarification and pre-purification of pDNA. In this sense, multi-walled carbon nanotubes were employed for solid-phase extraction in a complex matrix sample. The goal was to extract impurities like RNA, proteins, and gDNA, leaving a clarified pDNA sample, reducing the number of steps and time spent in downstream processes.

First, RNA adsorption assays were carried out to understand the optimal conditions to adsorb RNA. Experimental results suggest that the clarification process is associated with the diameter of carbon nanotubes, since to the smaller diameter corresponded a higher adsorption capacity. In this sense, MWCNTs with <10 nm of diameter were chosen with the best adsorption capacity. Moreover, from the study of the mechanism of interaction it was verified that RNA adsorption was mainly dependent on the hydrophobic interactions between the nitrogen bases of RNA and the aromatic surface of MWCNTs. This also led to preferred adsorption of single-stranded nucleic acids with more available exposed bases, as is the case of RNA, in comparison to pDNA. For the best performance of MWCNTs and to gain economic advantages, regeneration and reusability are key aspects to be evaluated. In this sense, a two-step desorption strategy was established, based on the use of 1 M NaOH after Tween-20 0.5%, and the regeneration and reuse of MWCNTs was successfully achieved. MWCNTs demonstrated good stability and efficiency throughout three adsorption cycles. Most importantly, when a complex *E. coli* lysate sample was applied, MWCNTs proved to have a great adsorption capacity even in a complex matrix, adsorbing all RNA present in the sample, with only three cycles, with no apparent pDNA capture. Actually, it was also verified that this methodology allows the recovery of pDNA in a stable form and with high recovery yield. The MWCNTs were also studied regarding their safety when in contact with a human cell line, and no cytotoxic effects have been observed. To better address the purity level of pDNA, it was studied the removal of other bacterial components that could cause immunogenicity, like proteins and gDNA. With these assays, it was verified that the clarification procedure could significantly reduce proteins in 41 % and gDNA in 84%.

Altogether, this work shows that as-grown MWCNTs can be considered a promising adsorbent for pDNA clarification. MWCNTs can be potentially used as a simple, efficient,

and reliable method for pDNA isolation from bacterial lysates, removing a vast amount of the major impurities present in the sample with a great adsorption capacity without using any organic solvent.

Although the great potential demonstrated by MWCNTs, further studies are still required. Thus, for future perspective, the work will focus on improving the desorption and regeneration of the carbon nanotubes by finding a milder desorption strategy that enables the recovery of RNA adsorbed with good integrity. It would also be interesting to explore more specific interactions between CNTs and nucleic acids by functionalization and conjugate this method with a possible delivery strategy.

CHAPTER 6

6.References

[1] R. P. Feynman, “There’s Plenty of Room at the Bottom,” 1960.

[2] “What is Nanotechnology? | nano.gov.” https://www.nano.gov/nanotech-101/what/definition (accessed Jan. 12, 2021).

[3] C. Buzea *et al.*, “Nanomaterials and nanoparticles: Sources and toxicity,” *Biointerphases*, vol. 2, no. 4, pp. MR17–MR71, 2007, doi: 10.1116/1.2815690.

[4] M. Nasrollahzadeh *et. al*, “An Introduction to Nanotechnology,” in *Interface Science and Technology*, vol. 28, pp. 1–27, 2019.

[5] M. Karimi *et al.*, “Carbon nanotubes part II: a remarkable carrier for drug and gene delivery,” *Expert Opin. Drug Deliv.*, vol. 12, no. 7, pp. 1089–1105, 2015, doi: 10.1517/17425247.2015.1004309.

[6] Y. Cao *et al.*, “Enhanced Lysosomal Escape of pH-Responsive Polyethylenimine-Betaine Functionalized Carbon Nanotube for the Codelivery of Survivin Small Interfering RNA and Doxorubicin,” *ACS Appl. Mater. Interfaces*, vol. 11, no. 10, pp. 9763–9776, 2019, doi: 10.1021/acsami.8b20810.

[7] A. Kordzadeh *et al.*, “Adsorption and encapsulation of the drug doxorubicin on covalent functionalized carbon nanotubes: A scrutinized study by using molecular dynamics simulation and quantum mechanics calculation,” *J. Mol. Graph. Model.*, vol. 88, pp. 11–22, 2019, doi: 10.1016/j.jmgm.2018.12.009.

[8] G. Biagiotti *et al.*, “Metformin salts with oxidized multiwalled carbon nanotubes: In vitro biological activity and inhibition of CNT internalization,” *J. Drug Deliv. Sci. Technol.*, vol. 47, pp. 254–258, 2018, doi: 10.1016/j.jddst.2018.07.023.

[9] H. Li *et al.*, “Preparation and properties of carbon nanotube (Fe)/hydroxyapatite composite as magnetic targeted drug delivery carrier,” *Mater. Sci. Eng. C*, vol. 97, pp. 222–229, 2019, doi: 10.1016/j.msec.2018.11.042.

[10] A. Burke *et al.*, “Long-term survival following a single treatment of kidney tumors with multiwalled carbon nanotubes and near-infrared radiation,” *Proc. Natl. Acad. Sci. U. S. A.*, vol. 106, no. 31, pp. 12897–12902, 2009, doi: 10.1073/pnas.0905195106.

[11] C. J. Gannon *et al.*, “Carbon nanotube-enhanced thermal destruction of cancer cells in a noninvasive radiofrequency field,” *Cancer*, vol. 110, no. 12, pp. 2654–

2665, 2007, doi: 10.1002/cncr.23155.

[12] F. Zhou *et al.*, "Mitochondria-targeting single-walled carbon nanotubes for cancer photothermal therapy," *Small*, vol. 7, no. 19, pp. 2727–2735, 2011, doi: 10.1002/smll.201100669.

[13] F. Zhou *et al.*, "Antitumor immunologically modified carbon nanotubes for photothermal therapy," *Biomaterials*, vol. 33, no. 11, pp. 3235–3242, 2012, doi: 10.1016/j.biomaterials.2011.12.029.

[14] J. Wan *et al.*, "A simple method for preparing biocompatible composite of cellulose and carbon nanotubes for the cell sensor," *Sensors Actuators, B Chem.*, vol. 146, no. 1, pp. 221–225, 2010, doi: 10.1016/j.snb.2010.02.037.

[15] F. L. Liu *et al.*, "Single-walled carbon nanotube-based biosensors for the detection of volatile organic compounds of lung cancer," *Phys. E Low-Dimensional Syst. Nanostructures*, vol. 44, no. 2, pp. 367–372, 2011, doi: 10.1016/j.physe.2011.08.033.

[16] C. Baj-Rossi *et al.*, "Electrochemical Detection of Anti-Breast-Cancer Agents in Human Serum by Cytochrome P450-Coated Carbon Nanotubes," *Sensors*, vol. 12, no. 5, pp. 6520–6537, 2012, doi: 10.3390/s120506520.

[17] S. Iijima, "Helical microtubules of graphitic carbon," *Nature*, vol. 354, no. 6348, pp. 56–58, 1991, doi: 10.1038/354056a0.

[18] J. Kaur *et al.*, "Applications of Carbon Nanotubes in Drug Delivery: A Comprehensive Review," in *Characterization and Biology of Nanomaterials for Drug Delivery: Nanoscience and Nanotechnology in Drug Delivery*, Elsevier, pp. 113–135, 2018.

[19] M. Monthioux *et al.*, "Carbon Nanotubes," in *Springer Handbooks*, pp. 193–247, 2017.

[20] A. Eatemadi *et al.*, "Carbon nanotubes: properties, synthesis, purification, and medical applications," *Nanoscale Res. Lett.*, vol. 9, no. 1, p. 393, 2014, doi: 10.1186/1556-276X-9-393.

[21] H. He *etal.*, "Carbon nanotubes: Applications in pharmacy and medicine," *Biomed Res. Int.*, vol. 2013, 2013, doi: 10.1155/2013/578290.

[22] N. Govindaraju and R. N. Singh, "Synthesis and Properties of Boron Nitride Nanotubes," in *Nanotube Superfiber Materials: Changing Engineering Design*,

Elsevier Inc., pp. 243–265, 2013.

[23] X. Wu *et al.*, "Recent progress in the synthesis of graphene/CNT composites and the energy-related applications," *Journal of Materials Science and Technology*, vol. 55. Chinese Society of Metals, pp. 16–34, 2020, doi: 10.1016/j.jmst.2019.05.063.

[24] V. C. Tung *et al.*, "Low-Temperature solution processing of graphene-carbon nanotube hybrid materials for high-performance transparent conductors," *Nano Lett.*, vol. 9, no. 5, pp. 1949–1955, 2009, doi: 10.1021/nl9001525.

[25] D. Danailov *et al.*, "Bending Properties of Carbon Nanotubes Encapsulating Solid Nanowires," *J. Nanosci. Nanotechnol.*, vol. 2, no. 5, pp. 503–507, 2002, doi: 10.1166/153348802760394089.

[26] R. P. Feazell *et al.*, "Soluble single-walled carbon nanotubes as longboat delivery systems for platinum(IV) anticancer drug design," *J. Am. Chem. Soc.*, vol. 129, no. 27, pp. 8438–8439, 2007, doi: 10.1021/ja073231f.

[27] C. Klumpp *et al.*, "Functionalized carbon nanotubes as emerging nanovectors for the delivery of therapeutics," *Biochimica et Biophysica Acta - Biomembranes*, vol. 1758, no. 3. Elsevier BV, pp. 404–412, 2006, doi: 10.1016/j.bbamem.2005.10.008.

[28] E. Bekyarova *et al.*, "Applications of Carbon Nanotubes in Biotechnology and Biomedicine," *J. Biomed. Nanotechnol.*, vol. 1, no. 1, pp. 3–17, 2006, doi: 10.1166/jbn.2005.004.

[29] H. He *et al.*, "Carbon nanotubes: Applications in pharmacy and medicine," *Biomed Res. Int.*, vol. 2013, 2013, doi: 10.1155/2013/578290.

[30] A. Thess *et al.*, "Crystalline ropes of metallic carbon nanotubes," *Science (80-.).*, vol. 273, no. 5274, pp. 483–487, 1996, doi: 10.1126/science.273.5274.483.

[31] L. Chico *et al.*, "Pure carbon nanoscale devices: Nanotube heterojunctions," *Phys. Rev. Lett.*, vol. 76, no. 6, pp. 971–974, 1996, doi: 10.1103/PhysRevLett.76.971.

[32] M. I. Sajid *et al.*, "Carbon nanotubes from synthesis to in vivo biomedical applications," *International Journal of Pharmaceutics*, vol. 501, no. 1–2. Elsevier B.V., pp. 278–299, 2016, doi: 10.1016/j.ijpharm.2016.01.064.

[33] P. Chandrasekhar, *Conducting Polymers, Fundamentals and Applications*. Springer International Publishing, 2018.

[34] V. Negri *et al.* , "Carbon Nanotubes in Biomedicine," *Topics in Current Chemistry*, vol. 378, no. 1. Springer, p. 15, 2020, doi: 10.1007/s41061-019-0278-8.

[35] M. S. Hasnain and A. K. Nayak, *Carbon Nanotubes for Targeted Drug Delivery*. Singapore: Springer Singapore, 2019.

[36] C. A. Dyke and J. M. Tour, "Covalent functionalization of single-walled carbon nanotubes for materials applications," *J. Phys. Chem. A*, vol. 108, no. 51, pp. 11151–11159, 2004, doi: 10.1021/jp046274g.

[37] T. Zhang *et al.*, "Polymeric Ruthenium Porphyrin-Functionalized Carbon Nanotubes and Graphene for Levulinic Ester Transformations into γ-Valerolactone and Pyrrolidone Derivatives," *ACS Omega*, vol. 2, no. 7, pp. 3228–3240, 2017, doi: 10.1021/acsomega.7b00427.

[38] L. Vaisman *et al.*, "The role of surfactants in dispersion of carbon nanotubes," *Advances in Colloid and Interface Science*, vol. 128–130. Elsevier, pp. 37–46, 21, 2006, doi: 10.1016/j.cis.2006.11.007.

[39] X. Zhou et al., "Supported lipid bilayer/carbon nanotube hybrids," *Nat. Nanotechnol.*, vol. 2, no. 3, pp. 185–190, 2007, doi: 10.1038/nnano.2007.34.

[40] S. Y. Niu *et al.*, "DNA/single-walled carbon nanotubes based fluorescence detection of Hg2+," *Anal. Lett.*, vol. 43, no. 15, pp. 2432–2439, 2010, doi: 10.1080/00032711003717455.

[41] T. L. Tran *et al.*, "Detection of influenza A virus using carbon nanotubes field effect transistor based DNA sensor," *Phys. E Low-Dimensional Syst. Nanostructures*, vol. 93, pp. 83–86, 2017, doi: 10.1016/j.physe.2017.05.019.

[42] C. Ge *et al.*, "Binding of blood proteins to carbon nanotubes reduces cytotoxicity," *Proc. Natl. Acad. Sci. U. S. A.*, vol. 108, no. 41, pp. 16968–16973, 2011, doi: 10.1073/pnas.1105270108.

[43] C. Richard *et al.*, "Noncovalent functionalization of carbon nanotubes with amphiphilic Gd 3+ chelates: Toward powerful T1 and T2 MRI contrast agents," *Nano Lett.*, vol. 8, no. 1, pp. 232–236, 2008, doi: 10.1021/nl072509z.

[44] S. Taghavi *et al.*, "Polyethylenimine-functionalized carbon nanotubes tagged with AS1411 aptamer for combination gene and drug delivery into human gastric cancer cells," *Int. J. Pharm.*, vol. 516, no. 1–2, pp. 301–312, 2017, doi: 10.1016/j.ijpharm.2016.11.027.

[45] M. R. Aires-Barros and A. M. Azevedo, “Fundamentals of Biological Separation Processes,” in *Current Developments in Biotechnology and Bioengineering: Foundations of Biotechnology and Bioengineering*, Elsevier Inc., pp. 187–237, 2017.

[46] Y.-C. Chen and M.-K. Yeh, “Introductory Chapter: Biopharmaceuticals,” in *Biopharmaceuticals*, InTech, 2018.

[47] D. F. Miguel Prazeres, “Plasmid Biopharmaceuticals: Basics, Applications, and Manufacturing,” 2011. [Online]. Available: www.wiley.com/go/permissions.

[48] G. Walsh, “Biopharmaceutical benchmarks 2018,” *Nat. Biotechnol.*, vol. 36, no. 12, pp. 1136–1145, 2018, doi: 10.1038/nbt.4305.

[49] B. Benyahia *et al.*, “Biopharmaceutical development, production, and quality,” in *New and Future Developments in Microbial Biotechnology and Bioengineering*, Elsevier, pp. 69–89, 2020.

[50] P. Gronemeyer *et al.*, “Trends in upstream and downstream process development for antibody manufacturing,” *Bioengineering*, vol. 1, no. 4. MDPI AG, pp. 188–212, 2014, doi: 10.3390/bioengineering1040188.

[51] A. Jungbauer, “Continuous downstream processing of biopharmaceuticals,” *Trends in Biotechnology*, vol. 31, no. 8. Elsevier Current Trends, pp. 479–492, 2013, doi: 10.1016/j.tibtech.2013.05.011.

[52] K. G. Clarke, “Downstream processing,” in *Bioprocess Engineering*, Elsevier, pp. 209–234, 2013.

[53] G. D. Najafpour, “Downstream Processing,” in *Biochemical Engineering and Biotechnology*, Elsevier, pp. 227–256, 2015.

[54] P. A. J. Rosa *et al.*, “Application of aqueous two-phase systems to antibody purification: A multi-stage approach,” *J. Biotechnol.*, vol. 139, no. 4, pp. 306–313, 2009, doi: 10.1016/j.jbiotec.2009.01.001.

[55] M. Ghorbani, M. Aghamohammadhassan, H. Ghorbani, and A. Zabihi, “Trends in sorbent development for dispersive micro-solid phase extraction,” *Microchem. J.*, vol. 158, p. 105250, 2020, doi: 10.1016/j.microc.2020.105250.

[56] H. Patel, “Fixed-bed column adsorption study: a comprehensive review,” *Appl. Water Sci.*, vol. 9, no. 3, p. 3, 2019, doi: 10.1007/s13201-019-0927-7.

[57] K. Vijayalakshmi *et al.*, “Batch adsorption and desorption studies on the removal

of lead (II) from aqueous solution using nanochitosan/sodium alginate/microcrystalline cellulose beads," *Int. J. Biol. Macromol.*, vol. 104, pp. 1483–1494, 2017, doi: 10.1016/j.ijbiomac.2017.04.120.

[58] A. Andrade-Eiroa *et al.*, "Solid-phase extraction of organic compounds: A critical review (Part I)," *TrAC - Trends in Analytical Chemistry*, vol. 80. Elsevier B.V., pp. 641–654, 2016, doi: 10.1016/j.trac.2015.08.015.

[59] C. Herrero Latorre *et al.*, "Carbon nanotubes as solid-phase extraction sorbents prior to atomic spectrometric determination of metal species: A review," *Anal. Chim. Acta*, vol. 749, pp. 16–35, 2012, doi: 10.1016/j.aca.2012.09.001.

[60] K. Xu *et al.*, "Solid-phase extraction of DNA by using a composite prepared from multiwalled carbon nanotubes, chitosan, Fe3O4 and a poly(ethylene glycol)-based deep eutectic solvent," *Microchim. Acta*, vol. 184, no. 10, pp. 4133–4140, 2017, doi: 10.1007/s00604-017-2444-4.

[61] M. J. Telepchak *et al.*, "Introduction to Solid Phase Extraction," in *Forensic and Clinical Applications of Solid Phase Extraction*, Humana Press, pp. 1–39, 2004.

[62] C. Baggiani *et al.*, "Solid phase extraction of food contaminants using molecular imprinted polymers," *Anal. Chim. Acta*, vol. 591, no. 1 SPEC. ISS., pp. 29–39, 2007, doi: 10.1016/j.aca.2007.01.056.

[63] J. C. Carlson *et al.*, "Stability of pharmaceuticals and other polar organic compounds stored on polar organic chemical integrative samplers and solid-phase extraction cartridges," *Environ. Toxicol. Chem.*, vol. 32, no. 2, pp. 337–344, 2013, doi: 10.1002/etc.2076.

[64] N. H. Packer *et al.,* "A general approach to desalting oligosaccharides released from glycoproteins," *Glycoconj. J.*, vol. 15, no. 8, pp. 737–747, 1998, doi: 10.1023/A:1006983125913.

[65] A. Zwir-Ferenc and M. Biziuk, "Solid phase extraction technique-trends, opportunities and applications," *Polish J. Environ. Stud.*, vol. 15, no. 5, pp. 677–690, 2006.

[66] L. Van Heukelem and C. S. Thomas, "Computer-assisted high-performance liquid chromatography method development with applications to the isolation and analysis of phytoplankton pigments," *J. Chromatogr. A*, vol. 910, no. 1, pp. 31–49, 2001, doi: 10.1016/S0378-4347(00)00603-4.

[67] Y. Wen *et al.*, "Recent advances in solid-phase sorbents for sample preparation

prior to chromatographic analysis," *TrAC - Trends in Analytical Chemistry*, vol. 59. Elsevier B.V., pp. 26–41, 2014, doi: 10.1016/j.trac.2014.03.011.

[68] V. Camel, "Solid phase extraction of trace elements," *Spectrochimica Acta - Part B Atomic Spectroscopy*, vol. 58, no. 7. Elsevier, pp. 1177–1233, 2003, doi: 10.1016/S0584-8547(03)00072-7.

[69] A. Andrade-Eiroa *et al.*, "Solid-phase extraction of organic compounds: A critical review. part ii," *TrAC - Trends in Analytical Chemistry*, vol. 80. Elsevier B.V., pp. 655–667, 2016, doi: 10.1016/j.trac.2015.08.014.

[70] C. F. Poole, "Core concepts and milestones in the development of solid-phase extraction," in *Solid-Phase Extraction*, Elsevier, pp. 1–36, 2020.

[71] W. kui Li and Y. ping Shi, "Recent advances and applications of carbon nanotubes based composites in magnetic solid-phase extraction," *TrAC - Trends in Analytical Chemistry*, vol. 118. Elsevier B.V., pp. 652–665, 2019, doi: 10.1016/j.trac.2019.06.039.

[72] M. Valcárcel *et al.*, "Role of carbon nanotubes in analytical science," *Analytical Chemistry*, vol. 79, no. 13. American Chemical Society , pp. 4788–4797, 2007, doi: 10.1021/ac070196m.

[73] P. C. Ma *et al.*, "Dispersion and functionalization of carbon nanotubes for polymer-based nanocomposites: A review," *Composites Part A: Applied Science and Manufacturing*, vol. 41, no. 10. Elsevier Ltd, pp. 1345–1367, 2010, doi: 10.1016/j.compositesa.2010.07.003.

[74] D. E. Hill *et al.*, "Functionalization of carbon nanotubes with polystyrene," *Macromolecules*, vol. 35, no. 25, pp. 9466–9471, 2002, doi: 10.1021/ma020855r.

[75] Y. Geng *et al.*, "Effects of surfactant treatment on mechanical and electrical properties of CNT/epoxy nanocomposites," *Compos. Part A Appl. Sci. Manuf.*, vol. 39, no. 12, pp. 1876–1883, 2008, doi: 10.1016/j.compositesa.2008.09.009.

[76] V. Georgakilas *et al.*, "Decorating carbon nanotubes with metal or semiconductor nanoparticles," *J. Mater. Chem.*, vol. 17, no. 26, pp. 2679–2694, 2007, doi: 10.1039/b700857k.

[77] O. Maslova *et al.*, "Gene therapy," in *Encyclopedia of Biomedical Gerontology*, Elsevier, pp. 136–146, 2019.

[78] L. Naldini, "Gene therapy returns to centre stage," *Nature*, vol. 526, no. 7573.

Nature Publishing Group, pp. 351–360, 2015, doi: 10.1038/nature15818.

[79] Y. Weng *et al.*, "Improved Nucleic Acid Therapy with Advanced Nanoscale Biotechnology," *Molecular Therapy - Nucleic Acids*, vol. 19. Cell Press, pp. 581–601, 2020, doi: 10.1016/j.omtn.2019.12.004.

[80] S. Worgall and R. G. Crystal, "Gene therapy," in *Principles of Tissue Engineering*, Elsevier, pp. 493–518, 2020.

[81] N. Brunetti-Pierri, "Gene therapy and gene editing," in *Handbook of Clinical Adult Genetics and Genomics*, Elsevier, pp. 463–477, 2020.

[82] H. Yin *et al.*, "Non-viral vectors for gene-based therapy," *Nature Reviews Genetics*, vol. 15, no. 8. Nature Publishing Group, pp. 541–555, 15, 2014, doi: 10.1038/nrg3763.

[83] K. Sridharan and N. J. Gogtay, "Therapeutic nucleic acids: current clinical status," *British Journal of Clinical Pharmacology*, vol. 82, no. 3. Blackwell Publishing Ltd, pp. 659–672, 2016, doi: 10.1111/bcp.12987.

[84] G. N. M. Ferreira, "Chromatographic approaches in the purification of plasmid DNA for therapy and vaccination," *Chemical Engineering and Technology*, vol. 28, no. 11. pp. 1285–1294, 2005, doi: 10.1002/ceat.200500158.

[85] K. Listner *et al.*, "Development of a highly productive and scalable plasmid DNA production platform," *Biotechnol. Prog.*, vol. 22, no. 5, pp. 1335–1345, 2006, doi: 10.1021/bp060046h.

[86] A. Abdulrahman and A. Ghanem, "Recent advances in chromatographic purification of plasmid DNA for gene therapy and DNA vaccines: A review," *Analytica Chimica Acta*, vol. 1025. Elsevier B.V., pp. 41–57, 2018, doi: 10.1016/j.aca.2018.04.001.

[87] Ç. Kip *et al.*, "Isolation of RNA and beta-NAD by phenylboronic acid functionalized, monodisperse-porous silica microspheres as sorbent in batch and microfluidic boronate affinity systems," *Colloids Surfaces B Biointerfaces*, vol. 174, pp. 333–342, 2019, doi: 10.1016/j.colsurfb.2018.11.012.

[88] S. Senel, "Boronic acid carrying (2-hydroxyethylmethacrylate)-based membranes for isolation of RNA," *Colloids Surfaces A Physicochem. Eng. Asp.*, vol. 219, no. 1–3, pp. 17–23, 2003, doi: 10.1016/S0927-7757(03)00007-4.

[89] L. L. Hu *et al.*, "Polyethyleneimine-iron phosphate nanocomposite as a promising

adsorbent for the isolation of DNA," *Talanta*, vol. 132, pp. 857–863, 2015, doi: 10.1016/j.talanta.2014.10.047.

[90] M. Ghaemi and G. Absalan, "Study on the adsorption of DNA on Fe3O4 nanoparticles and on ionic liquid-modified Fe3O4 nanoparticles," *Microchim. Acta*, vol. 181, no. 1–2, pp. 45–53, 2014, doi: 10.1007/s00604-013-1040-5.

[91] M. D. Rossell *et al.*, "Impact of sonication pretreatment on carbon nanotubes: A transmission electron microscopy study," *Carbon N. Y.*, vol. 61, pp. 404–411, 2013, doi: 10.1016/j.carbon.2013.05.024.

[92] R. Arrigo *et al.*, "Sonication-Induced Modification of Carbon Nanotubes: Effect on the Rheological and Thermo-Oxidative Behaviour of Polymer-Based Nanocomposites," *Materials (Basel).*, vol. 11, no. 3, p. 383, 2018, doi: 10.3390/ma11030383.

[93] R. J. Chen *et al.*, "Noncovalent sidewall functionalization of single-walled carbon nanotubes for protein immobilization ," *J. Am. Chem. Soc.*, vol. 123, no. 16, pp. 3838–3839, 2001, doi: 10.1021/ja010172b.

[94] A. Doepke *et al.*, "Analysis of the Electrochemical Oxidation of Multiwalled Carbon Nanotube Tower Electrodes in Sodium Hydroxide," *Electroanalysis*, vol. 24, no. 7, pp. 1501–1508, 2012, doi: 10.1002/elan.201200105.

[95] C. Kepka *et al.*, "Extraction of plasmid DNA from Escherichia coli cell lysate in a thermoseparating aqueous two-phase system," *J. Chromatogr. A*, vol. 1024, no. 1–2, pp. 95–104, 2004, doi: 10.1016/j.chroma.2003.10.028.

[96] J. Liu, "Adsorption of DNA onto gold nanoparticles and graphene oxide: Surface science and applications," *Physical Chemistry Chemical Physics*, vol. 14, no. 30. The Royal Society of Chemistry, pp. 10485–10496, 2012, doi: 10.1039/c2cp41186e.

[97] X. W. Chen *et al.*, "Isolation/separation of plasmid DNA using hemoglobin modified magnetic nanocomposites as solid-phase adsorbent," *Talanta*, vol. 100, pp. 107–112, 2012, doi: 10.1016/j.talanta.2012.07.095.

[98] R. W. Corbin *et al.*, "Toward a protein profile of Escherichia coli: Comparison to its transcription profile," *Proc. Natl. Acad. Sci. U. S. A.*, vol. 100, no. 16, pp. 9232–9237, 2003, doi: 10.1073/pnas.1533294100.

[99] S. Wang *et al.*, "Peptides with selective affinity for carbon nanotubes," *Nat. Mater.*, vol. 2, no. 3, pp. 196–200, 2003, doi: 10.1038/nmat833.

[100] M. A. Witek *et al.*, “Purification and preconcentration of genomic DNA from whole cell lysates using photoactivated polycarbonate (PPC) microfluidic chips,” *Nucleic Acids Res.*, vol. 34, no. 10, pp. e74–e74, 2006, doi: 10.1093/nar/gkl146.